


Summer 8-1-2017

# An Automated Device to Increase Screening Throughput of Zebrafish Larvae

Fuoad Saliou-Sulley

University of Maine, fssulley@gmail.com

Follow this and additional works at: <http://digitalcommons.library.umaine.edu/etd>

 Part of the [Biological Engineering Commons](#), [Biomedical Devices and Instrumentation Commons](#), and the [Other Biomedical Engineering and Bioengineering Commons](#)

---

## Recommended Citation

Saliou-Sulley, Fuoad, "An Automated Device to Increase Screening Throughput of Zebrafish Larvae" (2017). *Electronic Theses and Dissertations*. 2720.

<http://digitalcommons.library.umaine.edu/etd/2720>

This Open-Access Thesis is brought to you for free and open access by DigitalCommons@UMaine. It has been accepted for inclusion in Electronic Theses and Dissertations by an authorized administrator of DigitalCommons@UMaine. For more information, please contact [um.library.technical.services@maine.edu](mailto:um.library.technical.services@maine.edu).

**AN AUTOMATED DEVICE TO INCREASE SCREENING THROUGHPUT OF  
ZEBRAFISH LARVAE**

By

Fuoad Saliou-Sulley

B.S. University of Maine, 2014

A THESIS

Submitted in Partial Fulfillment of the

Requirements for the Degree of

Master of Science

(in Biological Engineering)

The Graduate School

The University of Maine

August 2017

Advisory Committee:

Paul J. Millard, Associate Professor of Chemical and Biological Engineering,

Advisor

Douglas W. Bousfield, Professor of Chemical and Biological Engineering

Sara Walton, Lecturer, Chemical and Biological Engineering

© 2017 Fuoad Saliou-Sulley

All Rights Reserved

**AN AUTOMATED DEVICE TO INCREASE SCREENING THROUGHPUT OF  
ZEBRAFISH LARVAE**

By Fuoad Saliou-Sulley

Thesis Advisor: Dr. Paul Millard

An Abstract of the Thesis Presented

in Partial Fulfillment of the

Requirements for the

Degree of Master of Science

(in Biological Engineering)

August 2017

The use of the zebrafish as an animal model alternative to mammalian species has spawned research advancements in several medical fields<sup>1</sup>. Since the zebrafish shares a high degree of sequence and functional homology with mammals, studies using this organism can provide in-depth insight into host response to disease and provide a platform for testing a range of treatment options. The optical transparency of zebrafish at early stages of development permits easy assessment of the effects of treatments, occurrence of tumors or other abnormal growth, disease progression, and immune response. These characteristics make it ideal for studying human diseases such as the Influenza A Virus (IAV). The conventional method of IAV transmission is by aerosol, and since the zebrafish does not accommodate this mode of entry, the virus is injected into the specimen under study.

The larvae typically require manipulation during preparatory procedures prior to assessment, a process that can be time consuming and stressful for the organism.

In this thesis, I describe the development of a device designed to eliminate problems associated with manipulating zebrafish larvae by automatically conducting specimen from a reservoir directly into an entrapment dock, where it will be immobilized for injection and rapidly removed post-injection. This will help to reduce the handling time of large sample sets, thereby increasing the screening throughput. Zebrafish have fast growth rates<sup>4</sup> hence preparatory procedures for analysis like injection should be as quick and efficient as possible. The device uses a system to conduct 48-72 hour old zebrafish through a liquid medium (egg water) using a syringe pump. The complete system consists of three main subsystems, namely the pump, optical detection and entrapment components. A 3D printed housing encloses the electrical components of the entire system. The device works by aspirating individual fish through a tube via a pressure gradient created with a syringe pump. Each cycle of the device involves the following steps: (1) loading, (2) sensing, (3) trapping, (4) injection, and (5) flushing. During loading, a single larva is extracted from the reservoir and conducted through a tube past the optical detection subsystem. At the sensing stage, the optical detection subsystem composed of a photodiode and a laser, senses transmitted light from the laser and discerns the entry of larva from air bubbles and debris with precision. Upon larva recognition, the specimen is then conducted to the entrapment dock (step 3) where it will be immobilized for injection (step 4). The final step (5) involves conducting

the larva out of the entrapment dock and subsequently out of entire system for further analysis. This device will primarily serve zebrafish researchers who intend to introduce vaccines, pathogens and other experimental materials into many individual zebrafish larvae.

## **ACKNOWLEDGEMENTS**

I would like to use this opportunity to thank my thesis advisor, Dr. Paul Millard, for welcoming me into his lab and for being my mentor over the past few years. Through his support, my grasp for the subject has improved vastly and I am very grateful for his patience and guidance. I would also like to thank Dr. Doug Bousfield and Dr. Sara Walton for providing valuable contributions to this work. Additionally I would like to thank Sean Michael Taylor from the IMRC for providing critical design contributions and for helping me to become familiar with the prototyping equipment. I would also like to acknowledge Madeline Mazjanis for helping with the control software and for conducting device tests.

With a great deal of gratitude, I would like to thank my family for their continuous support in my endeavors. They have always believed in me and encouraged me to be the best version of myself and to never give up on my dreams, I will forever be grateful for their support.

## TABLE OF CONTENTS

ACKNOWLEDGEMENTS.....	iii
LIST OF TABLES.....	vii
LIST OF FIGURES.....	viii
CHAPTER 1. LITERATURE REVIEW.....	1
1.1 Influenza Virus Overview.....	1
1.2 Influenza Virus Variants.....	1
1.2.1 Epidemiology- IAV.....	2
1.2.2 IAV Transmission and Viral Propagation.....	3
1.2.3 Clinical Features of infection.....	5
1.3 Current IAV Research.....	5
1.4 Animal Models.....	6
1.4.1 Zebrafish as An Influenza A Virus Model.....	7
1.4.2 Pathological Phenotype Observed in IAV Infected Zebrafish.....	10
1.5 Systemic IAV Infection.....	11
1.5.1 $\alpha$ 2,6-linked Sialic Acids in Zebrafish.....	14
1.6 Zebrafish Antiviral Defenses.....	16
1.7 Injection of Zebrafish Embryos.....	17
1.7.1 Standard Techniques.....	21
1.7.2 Rapid Prototyping and Influence of Technology on Research.....	21
1.7.3 Notable Devices for Zebrafish Injection.....	22



CHAPTER 2. METHODS.....	27
2.1 Overview.....	27
2.2 Pump Subunit Components.....	29
2.3 Optical Detection Subunit Components.....	31
2.4 Entrapment Dock.....	32
2.4.1 Biocompatibility.....	37
2.5 Specifications and Parameters.....	38
2.6 Electronics.....	38
2.6.1 Control Maps/ Software Programming.....	42
 CHAPTER 3. EXPERIMENTAL RESULTS AND DISCUSSION.....	 46
3.1 Input Reservoir Efficacy Test.....	46
3.1.1 Procedure.....	46
3.1.2 Results.....	46
3.2 Optical detection Unit Efficacy Test.....	48
3.2.1 Procedure.....	48
3.2.2 Results.....	49
3.3 Entrapment Dock Tests.....	50
3.3.1 Procedure.....	50
3.4 Average Duration of Screening Steps (1 Cycle).....	51
3.4.1 Procedure.....	51
3.5 Quantitative Assessment of Animal Health.....	53
3.5.1 Procedure.....	53
3.5.2 Results.....	53

CHAPTER 4. SUMMARY, CONCLUSION AND FUTURE WORK.....	56
4.1 Summary.....	56
4.2 Conclusions.....	56
4.3 Future Work.....	57
BIBLIOGRAPHY.....	60
APPENDIX A: ZEBRAFISH HUSBANDRY.....	71
APPENDIX B: VALVE/SYRINGE PUMP CONTROL MAP.....	73
APPENDIX C: MATERIALS LIST.....	75
BIOGRAPHY OF THE AUTHOR.....	77

## LIST OF TABLES

Table 1.	Average duration of screening steps from the reservoir to the light detector at different flow rates. (0.08cm inner diameter and 88cm length).....	52
Table 2.	Calculated duration of screening steps from the photo-detector to the entrapment dock at different flow rates. (0.08cm inner diameter and 80cm length).....	52
Table 3.	Average time required for injection.....	52
Table 4.	Calculated duration of screening steps from the entrapment dock to the exit (of the entire system) at different flow rates. (0.08cm inner diameter and 62cm length).....	52

## LIST OF FIGURES

Figure 1.	Process of influenza virus infection.....	13
Figure 2.	A typical micromanipulator for manual injection needle operation in all three axes (x, y and z).....	20
Figure 3.	Device schematic and design.....	28
Figure 4.	An image of the input reservoir.....	29
Figure 5.	Aqua Culture single outlet aquarium air pump.....	30
Figure 6.	New Era NE-1000x bidirectional programmable syringe pump.....	31
Figure 7.	An image of the optical detection unit components.....	32
Figure 8.	Image of the entrapment dock with highlighted channels and dimensions in millimeters.....	33
Figure 9.	Images of the entrapment dock and its supporting components designed using solid edge cad software.....	36
Figure 10.	Electronic components.....	39
Figure 11.	Cole-Parmer two-way normally closed solenoid pinch valve.....	40
Figure 12.	Image of the functional circuit diagram of the voltage comparator....	42
Figure 13.	LabVIEW control dashboard.....	43
Figure 14.	Valve/syringe pump control map.....	44
Figure 15.	A bar graph depicting the number of zebrafish larvae collected after 60 sec at different flow rates.....	48
Figure 16.	A waveform chart of the photodiode voltage spikes with respect to time.....	50

Figure 17. Image of the entrapment dock illustrating the immobilized zebrafish larvae in the two possible orientations.....51

Figure 18. Comparison of morphological abnormalities of experimental zebrafish, at different flow rates, with a control zebrafish.....54

Figure 19. Quantitative assessment of zebrafish health at different flow rates (n=100).....55

## CHAPTER 1

### LITERATURE REVIEW

#### 1.1 Influenza Virus Overview

The contagious, acute respiratory illness known as the flu has afflicted humans for centuries, yet its precise origin remains a mystery. The working hypothesis is that wild aquatic birds were the primary reservoir for both bird and mammalian virus species. There is extensive evidence for the direct and indirect transmission of influenza from birds to other species such as pigs and horses<sup>5</sup>. Influenza viruses belong to the Orthomyxoviridae family of RNA viruses which affect the upper and lower respiratory tract. They are spherical or filamentous and range in size from 80 to 120 nm in diameter<sup>6,7</sup>. General symptoms of influenza include fever, malaise, headache and cough<sup>8</sup>. The disease affects all age groups but has high prevalence in people under 25 years and has more drastic and life threatening effects in infants and the elderly<sup>9,7,10,11</sup>. Flu outbreaks appear suddenly and can persist for a few days to months, if uncontrolled. The severity of an outbreak may vary depending on the variant of influenza virus causing the disease.

#### 1.2 Influenza Virus Variants

There are six genera within the Orthomyxoviridae virus family, and three, Influenza A, Influenza B and Influenza C, contain viruses that can cause influenza in humans and birds, as well as other mammals<sup>12,13</sup>. These variants are characterized by segmented negative strand-RNA genomes that are typically enclosed in a lipid envelope. Subtle classifications distinguish the three subfamilies. Viral surface

proteins serve as unique identification markers for viruses, and typical surface proteins include: a hemagglutinin (HA), which agglutinates erythrocytes and plays a key role in viral propagation, neuraminidase (NA), which is an enzyme essential for the release of progeny virus particles from the surface of an infected cell, and membrane (M) proteins, which serve as ion channels.

### **1.2.1 Epidemiology- IAV**

The most prevalent form of influenza is influenza A, which primarily affects humans, other mammals and birds. Influenza A is a disease of immense complexity. Its occurrence and outcome depend on interactions between the virus, which is constantly changing its genetic and antigenic composition, and the immune system of the host, which may not be able to respond adequately within a restricted time frame. The principal factor determining whether influenza outbreaks occur is the degree of complementary pairing between the surface antigens (HA and NA) of the virus and the antibodies against them, which are in the current population<sup>7</sup>. This class of viruses is the most lethal of the three (Influenza A, Influenza B and Influenza C), with the ability to cause severe diseases on the pandemic scale. Pandemics of influenza A have occurred about three times per century since 1700 and were manifested by global spread of the disease, typically with high morbidity and mortality<sup>14</sup>. The most extreme pandemic recorded in the 20<sup>th</sup> century was the Spanish influenza, prevalent between 1918 and 1919, with a death toll estimated to have been between 20 and 40 million people across the globe<sup>7,14</sup>. Other recent notable pandemics include the 2009 avian flu (H1N1) pandemic; this virus

was a unique combination of influenza virus genes never previously identified in either animals or people, infecting millions and killing thousands worldwide<sup>15</sup>.

For several decades, the Centers for Disease Control and Prevention (CDC) has made annual estimates of influenza-associated deaths, which have been used in influenza research to develop influenza control and prevention policy. Out of the 5-20% of people that contract the flu in the United States each year, the CDC estimates over 20,000 laboratory-confirmed hospitalizations annually, due to IAV and other related complications<sup>16,17</sup>. In addition, the economy is burdened by about 87 billion USD due to IAV related issues, ranging from medical expenses, paid work absences, losses in productivity, decline in retail spending, and even tourism<sup>18</sup>.

### **1.2.2 IAV Transmission and Viral Propagation**

The flu is highly contagious and infected people can spread it via aerosol to others up to about 6 feet away. The virus spreads mainly through tiny aerosol droplets produced when infected individuals cough, sneeze or, occasionally, just talk. The aerosol droplets containing the virus enter the mouth, nose or respiratory tract of people within proximity. In addition, the virus can be contracted when people come into direct contact with surfaces and objects contaminated with the virus and then later touch their mouth, nose, or eyes. Contaminated surfaces may include door handles, table surfaces, banknotes, and electronic input devices like keyboards. Research has proven that IAV can survive on such surfaces for up to eight hours<sup>19,20,21</sup>. The flu can be contagious even before symptoms become apparent. Most adults can infect others beginning one day before their symptoms of



the disease are displayed and can remain contagious for up to one week after becoming sick<sup>19</sup>. Young children with weakened immune systems, however, can be contagious well past a week.

Upon infection, the virus replicates in the upper and lower respiratory tract, reaching its peak at 2-3 days after infection. Symptoms of the disease start to become apparent at this stage<sup>19</sup>. The virus induces pathologic changes throughout the respiratory tract, with the most significant pathology occurring in the lower respiratory tract. Bronchoscopies of persons with the flu show a diffuse involvement of the trachea, larynx and the bronchi, with acute mucosal inflammation and edema. The virus has an affinity for cells in the epithelial lining of the respiratory mucosa. For viral propagation to initiate, infection of these cells must occur. Infection begins by virus binding to the surface of the host cell, followed by the fusion of viral and host cell membranes. The attachment and fusion is mediated by virus hemagglutinin glycoprotein (HA) interacting and binding to sialic acid cell receptors. Binding to sialic acid occurs via a shallow cavity near the distal tip of the HA glycoprotein. Subsequently, influenza virus enters the cell by receptor-mediated endocytosis<sup>22</sup>. Since the virus has no need for DNA coding, transcription occurs within the nucleus, followed by: replication of viral RNA and secondary transcription, translation of viral RNA to produce viral proteins, then culminating with the assembly of viral structural components and the release of progeny virus into the extracellular medium.

### **1.2.3 Clinical Features of Infection**

In humans, influenza is characterized by the sudden onset of an acute respiratory illness accompanied by headaches, chills and nonproductive cough. This is usually followed by muscle aches, high fever, generalized weakness and loss of appetite. The fever usually declines by the third day and is gone after about a week, but the coughing and signs of weakness can persist for about two more weeks<sup>10</sup>. Due to the virus' nature of compromising the immune system, the host can be prone to infection by other pathogens that can lead to further complications. Complications of the flu can include ear infections, sinus infections, dehydration, and worsening of chronic medical conditions such as congestive heart failure or diabetes. More severe illnesses such as primary influenza pneumonia can develop, which can be lethal. Secondary bacterial pneumonia, a more rare form of the disease, can also occur if the flu goes untreated<sup>23</sup>. People over 65 years of age, those with heart conditions, asthma, emphysema, AIDS or people receiving chemotherapy are at an increased risk of complications from influenza.

### **1.3 Current IAV Research**

Influenza A viruses, due to their genetic makeup and mode of propagation, are continuously changing in several animal hosts, including birds, pigs, horses and humans<sup>24</sup>. As a result of the rapid and constant emergence of new viral strains, IAV is highly likely to cause human epidemics. It is, however, necessary that naturally occurring IAV should be monitored and characterized to improve the current understanding of the host tropism as well as the virulence of IAV. There have been

numerous research advancements in IAV research in the past few decades, some of which include, but are not limited to: viral/human surveillance and characterization, influenza genome diversity of evolution, vaccination technologies, tissue pathology and influenza animal model manipulation technologies<sup>24,25,26,27,28,29,30</sup>. The National Institute of Allergy and Infectious Disease (NIAID) Influenza Research Program supports research to learn more about the structure and pathogenesis of influenza viruses. Such research has proven to be invaluable to the development of new vaccines, therapeutics, and diagnostics<sup>31</sup>. Current research involves understanding viral replication, the emergence of new viral strains and the effect those have on the immune system. A major NIAID activity is the Influenza Genome Sequencing Project. This is a joint effort to obtain complete genetic footprints of thousands of human and avian influenza strains, with the goal of providing valuable genomic knowledge that can be used to create improved public health countermeasures. As of May 2014, more than 16,000 human and avian isolates have been completely sequenced and made publicly available<sup>32</sup>.

NIAID also supports the research community by developing new animal models for preclinical evaluation of vaccine and therapeutic candidates. Animal models are useful tools that serve as biological resources for microarrays, clones, peptides, and reagents.

#### **1.4 Animal Models**

Animal models have been pivotal in research for decades, leading to major drug discoveries and medical breakthroughs<sup>33,34</sup>. Suitable models are usually

selected based on physiological, anatomical and genetic resemblance with humans. The unlimited supply and ease of manipulation are some of the general advantages of animal models. Scientific research can sometimes involve statistical analysis of test specimens, mostly by manipulating only one variable while keeping others constant, and then observing the consequences of that change. An adequate number of test specimens are, however, required to accomplish this task effectively. The relative ease of manipulating large sample sizes makes animal models invaluable to medical research.

Rodents are the most common type of mammal used in experimental studies. Extensive research has been conducted using rats, mice, gerbils, guinea pigs, and hamsters<sup>35,36</sup>. Among these rodents, the majority of genetic studies, especially those involving disease, have employed mice because their genomes are similar to that of humans and many unique strains have been developed. Other common experimental organisms include fruit flies, baker's yeast and zebrafish<sup>37</sup>.

#### **1.4.1 Zebrafish as An Influenza A Virus Model**

Animal models of influenza are essential to research that focuses on gaining a better understanding of the virus and its effect on humans. There are currently various research applications of animal models ranging from the pathogenesis and host response to IAV to antiviral drug screenings and pre-clinical testing of antiviral drugs and vaccines. IAV animal models are also used to investigate the competency of vaccines and drugs to combat the virus, prevent future complications and commonly, to reduce the symptoms of influenza. In selecting the models for

research, a couple of factors have to be considered. The most important criterion is the susceptibility of the animal to influenza virus infection while supporting viral replication, and exhibiting human histopathological and morphological symptoms of an influenza virus infection<sup>38</sup>.

Zebrafish (*Danio rerio*) models for infectious diseases are well established for characterization of bacterial, fungal and viral infections<sup>39,40,41</sup>. The National Institutes of Health (NIH) along with other research bodies has approved the zebrafish animal model for use in the advancement of biomedical studies. Some of its inherent advantages, such as optical transparency, minimal husbandry, large clutch size and fast reproductive cycle make the zebrafish an ideal specimen for high-throughput drug testing. Another important factor to consider is that zebrafish are propagated at the optimal incubation temperature for viruses during infection studies. Zebrafish can be grown in a temperature range within that of the human respiratory tract (from 25 to 33°C).

As a result, the zebrafish might be well suited to modeling human respiratory viral infections, given the similarities between the zebrafish swim bladder and the human lung<sup>42,43,44,45</sup>. There have also been recent studies of zebrafish swim bladder infections with human fungal pathogens. Furthermore, zebrafish at the early stage of development are highly amenable to genetic manipulation and transgenesis<sup>2</sup>.

Among all of the benefits of the zebrafish animal model system, one of the most important characteristics that make this system ideal for IAV research is the zebrafish's immune system. During the onset of development, zebrafish are known to rely solely on the innate immune response for the first 4 to 6 weeks<sup>46,47,48</sup>.

Hematopoiesis in zebrafish produces largely the same differentiated cell types as observed in mammals. Monocytes, neutrophils, macrophages and eosinophils have all been described within the zebrafish myeloid lineage<sup>47</sup>. In addition, other cells with mammalian cytotoxic properties, such as mast cells and natural killer cells, have also been classified within zebrafish<sup>49</sup>. The innate immune functions of these cells provide an effective defense system during the early stages of development<sup>50</sup>.

The majority of the research conducted using the zebrafish model involves fish-specific viral pathogens that have the ability to infect and cause disease; however, few human viruses have been demonstrated to infect the zebrafish<sup>51</sup>. Some recent studies have proven the zebrafish to be susceptible to viral infection by mammalian viruses, as characterized by Burgos *et al*, where the zebrafish was used as a model of herpes simplex virus type 1 (HSV-1) infection of the nervous system<sup>52</sup>.

Gabor *et al*, at the University of Maine described a zebrafish model for human influenza A Virus (IAV) infection and showed that zebrafish embryos are susceptible to infection with both influenza A strains APR8 and X-31 (Aichi). Influenza-infected zebrafish showed an increase in viral burden and mortality over time. The expression of innate antiviral genes, the gross pathology and the histopathology in infected zebrafish recapitulate clinical symptoms of influenza infections in humans<sup>2</sup>. The study was conducted based on the premise that an antiviral state similar to that in humans was induced in infected specimens, leading to the deduction that zebrafish can be a suitable alternative to vertebrate animal models used for IAV studies. Recombinant influenza viruses carrying a GFP reporter gene in the NS segment (NS1-GFP) were used to characterize infection in the zebrafish. Although

attenuated compared to the wild type virus, it is typical for these modified viral strains to replicate efficiently<sup>53</sup>. To determine whether the modified human isolates of IAV could cause disease in zebrafish embryos, different strains of IAV [APR8 (H1N1) and X-31 (H3N2)] were injected intravenously into 48 hpf (hours post fertilization) zebrafish through the Duct of Cuvier to mimic viral infection in the human blood stream. An inert phosphate buffered saline solution was also injected into a number of zebrafish embryos in a control setup<sup>2</sup>.

Data from the study demonstrated that IAV replicates within zebrafish and suggests that the death of IAV-infected zebrafish is likely to be caused by IAV infection. To investigate the effect of treatment on the zebrafish immune system, an antiviral compound used for the treatment of IAV in humans was introduced, which reduced the mortality of the infected fish as well as the virulence of IAV.

#### **1.4.2 Pathological Phenotype Observed in IAV Infected Zebrafish**

In an effort to characterize the innate immune response of zebrafish to the presence of either strain of IAV (APR8 or X-31) in the bloodstream, infected embryos were monitored over time for behavioral and phenotypic changes<sup>2</sup>. A controlled set of embryos were injected with PBS (phosphate-buffered saline) and monitored under identical conditions. While fish in the control setup displayed no abnormal behavior or signs of viremia, the IAV-injected zebrafish exhibited symptoms of lethargy, with signs of edema observed in the pericardium and yolk sac. Furthermore, the edema worsened over time and additional pathological phenotypes, including varying degrees of lordotic curvature of the spine, were

observed. Other observations included pigmentation defects, cranial irregularities and eye deformities.

Gabor *et al* extended the investigation to further characterize the innate immune response of zebrafish to IAV infection by conducting pathological analysis on the cellular level. Influenza virus typically replicates in the epithelial cells throughout the respiratory tract of humans and, the virus can be recovered from both the upper and lower respiratory tract of individuals who have been naturally or experimentally infected. IAV viremia in its acute stage can be characterized by multifocal destruction and desquamation of the pseudostratified columnar epithelium of the trachea and bronchi<sup>29</sup>. It is also typical for the basal layer of the epithelium to be the only structure remaining. Edema and congestion of the submucosa can also be observed.

In the case of the zebrafish, Gabor *et al.* prepared tissue samples from IAV infected zebrafish 48 after injection. Analysis of the tissues confirmed the clinical symptoms of influenza, including necrotic tissues and edema.

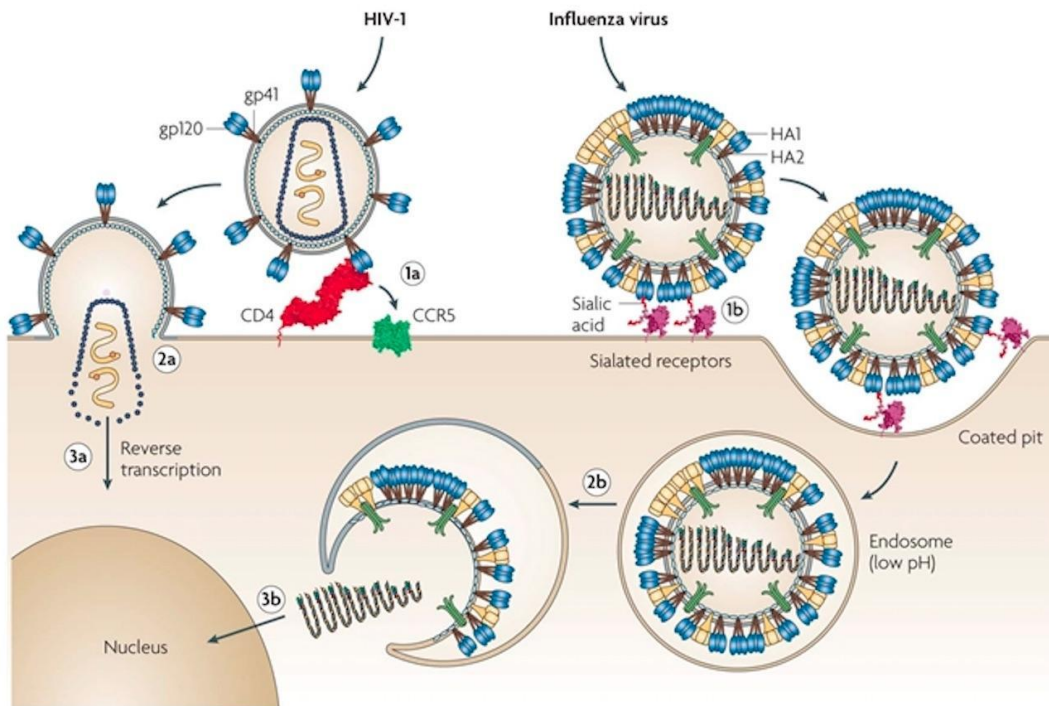
## **1.5 Systemic IAV Infection**

The vascular system allows the flow of blood from the heart to all parts of the body, supplying oxygen to the most vital organs such as the kidneys, the brain and the liver. Since blood within this system is distributed throughout the body from the aorta, introduction of a blood borne pathogen such as IAV into the vasculature expedites viral infection throughout the body. IAV is characterized by hemagglutinin (HA), an antigenic glycoprotein usually found on their surfaces. These glycoproteins



are responsible for binding the virus to the cell that is being infected<sup>54</sup>. The viral hemagglutinin proteins bind to sialic acid groups of cellular surface glycoproteins to achieve viral attachment and entry. The specificity of the HA-Sialic binding complex is one of the major determinants for controlling viral tropism and host specificity. This explains why some organisms are susceptible to certain disease-causing pathogens, while others are not.

Typically, human influenza viruses have a binding preference for  $\alpha$ 2,6-linked sialic acid. Avian influenza virus, on the other hand, binds to the  $\alpha$ 2,3-linked sialic acid of the host bird<sup>56</sup>. Besides the conventional viral infection mechanism, the virus can sometimes travel to acidic endosomes for membrane fusion via clathrin or caveolin mediated endocytosis<sup>57</sup>. Alternate pathways into the cell by viruses have also been studied, demonstrating that influenza viruses have the ability to employ different cell entry mechanisms to achieve viral infection. It is, however, not known whether all influenza viruses have the ability to use the other various pathways with identical preferences<sup>56, 58, 59, 60</sup>. Following the interaction between the viral HA and the  $\alpha$ 2,6-linked sialic acid, endocytosis of the viral particle is triggered. *Figure 1* demonstrates a typical process of cell entry of two different viruses: Influenza and HIV.



**Schematic diagrams of HIV-1 and influenza virus fusion and entry processes.** Major conformational changes in the viral envelope glycoproteins occur for fusion of both HIV-1 and influenza virus, but the requirements for fusion differ, as do the viral target types (not shown). For HIV-1, gp120 binds sequentially to its primary receptor CD4 and, after an initial conformational change, to co-receptors (chemokine receptor) CCR5 or CXCR4 (not shown) (step 1a). Co-receptor interaction triggers fusion of the viral and cellular membranes, initiated by the HIV-1 fusion peptide that is located in gp41 (step 2a). Fusion and entry of the HIV-1 genomic RNA and accompanying viral proteins into the target cell occurs at the cell surface at neutral pH. Following entry, the HIV-1 RNA genomes are transcribed by reverse transcriptase into DNA (step 3a) and the HIV-1 pre-integration complex is transported to the nucleus for integration into target cell genomic DNA to initiate chronic infection. On different cell types from those affected by HIV-1, influenza virus binds via haemagglutinin 1 (HA1) to terminal sialic acids present on glycoproteins or on glycolipids (step 1b). The virus is subsequently internalized by receptor-mediated endocytosis into a low pH compartment (endosome), triggering conformational changes that expose the viral fusion peptide that is located in HA2 (step 2b). Subsequently, the genomic ribonucleoprotein complex is transported to the nucleus to initiate transcription and replication of the viral genome (step 3b).

Figure 1: Process of influenza virus infection.

Karlsson et al. Schematic diagrams of HIV-1 and influenza virus fusion and entry processes. Diagram. The challenges of eliciting neutralizing antibodies to HIV-1 and to influenza virus. Fall 2008; 6(2): 148. Available from Nature Reviews Microbiology. Accessed May 6 2017.

Influenza virus binds to terminal sialic acids present on glycoproteins or glycolipids via HA1. The virus is subsequently internalized by receptor-mediated endocytosis into an endosome. This initiates conformational changes that expose the viral fusion peptide located on HA2. The entire viral protein complex is then transported to the nucleus, where transcription and replication of the viral genome will occur

Replication and translation of the viral RNA produces new viral macromolecules, which are ultimately assembled into complete viral particles for release and infection of new cells<sup>62</sup>.

### **1.5.1 $\alpha$ 2,6-linked Sialic Acids in Zebrafish**

The presence of compatible sialic acid modifications on host glycolipids or glycoproteins is one of the main determinants of viral infection in most animal species. The presence of  $\alpha$  2,6-linked sialic acid in the zebrafish makes this a valuable model system for the study of the influenza A virus. In spite of this, there are no known reported naturally occurring viral infections of the zebrafish<sup>63</sup>. In an effort to determine whether zebrafish embryos could serve as a host for infection with mammalian/human isolates of IAV, Gabor conducted a study to analyze the sialic acid linkage types present on zebrafish glycoproteins or glycolipids<sup>2</sup>. Analysis using High Performance Anion Exchange Chromatography with Pulsed Amperometric Detection (HPAEC-PAD) demonstrated that  $\alpha$  2,6-linked sialic acids were present in zebrafish embryos two days after fertilization. There were, however, no  $\alpha$  2,3-linked sialic acids detected in the two day-old embryos<sup>2</sup>. There

are a number of chemical variants of sialic acids, and influenza strains vary in their affinity for them. Terminally linked sialic acids can occur in  $\alpha$ -2,3,  $\alpha$ -2,6, or  $\alpha$ -2,8 linkages. Even though the study was not intended to identify  $\alpha$  2,8-linked sialic acids, others have previously demonstrated that zebrafish have the ability to synthesize a variety of sialylated glycoconjugates during the onset of their development<sup>64,65,66</sup>. These unique characteristics of the zebrafish model system make it an attractive candidate for studying infectious viral diseases. With further studies into sialylated glycoconjugates present at various stages of development of the zebrafish, additional human viral diseases can further be characterized. Some of the known human viral pathogens that have an affinity for  $\alpha$  2,6-linked sialic acids include certain members of the following virus families: coronaviridae, paramyxoviridae, caliciviridae, picornaviridae, reoviridae, polyomaviridae, adenoviridae and parvoviridae. Most of these groups contain major pathogens for humans that affect all parts of the body, ranging from small organs like the salivary gland (in the case of mumps) to cellular networks as intricate as the immune system<sup>2,67,68</sup>.

Avian influenza virus strains have the tendency to bind to sialic acids attached to galactose via an  $\alpha$  2,3-linkage, which is the major sialic acid on epithelial cells of the duck gut. Ciliated epithelial cells in the human trachea lack  $\alpha$  2,3 linked sialic acids, suggesting that the lack of a suitable receptor accounts for the inefficient replication of certain human viruses in duck intestine and of certain avian viruses in humans<sup>55,69</sup>.

## 1.6 Zebrafish Antiviral Defenses

Although the zebrafish animal model has been proven effective for testing medical treatments and virological assays, it can serve as an ideal tool for understanding host biological responses after viral infections, particularly the Influenza A virus. A clear and thorough understanding of a host's immunity (both innate and adaptive) can provide insight into new treatments and effective therapies. The zebrafish, like many organisms possesses innate and adaptive immunity, however the zebrafish relies solely on its innate immune response system for the first 4-6 weeks of development<sup>2</sup>. Within this period of growth, zebrafish develop from the embryo to the larvae stage. This temporal separation of innate and adaptive immunity in zebrafish allows for the study of the innate immune response to viral infection independent of adaptive immunity. Upon viral attack, one of the primary processes initiated is the induction of host antiviral state, which slows down the rate of progression of viremia<sup>2</sup>. The major molecule responsible for the antiviral state is interferon (IFN). Cells that are already infected with a virus secrete interferons to prevent further virus exposure of healthy cells. Response to IFN involves a rapid and direct signal transduction mechanism that quickly reports the presence of extracellular cytokines to the cell nucleus. This preserves the specificity inherent in cytokine-receptor interactions to induce expression of a set of genes via transcription, leading to encoding of important antiviral proteins. Establishment of the resulting antiviral state provides a crucial initial line of defense against viral infection. Studies of IFN-deficient cells and animals derived by gene targeting have demonstrated the essential nature of IFN-

mediated innate immunity<sup>70,71,72</sup>.

All blood cells in humans begin as hematopoietic stem cells, and then differentiate into myeloid cells (erythrocytes, megakaryocytes, monocytes, neutrophils, basophils, or eosinophils) or lymphoid cells (T-lymphocytes and B-lymphocytes). These immune cells typically perceive and respond to microbial stimuli. Zebrafish are largely similar to humans with respect to cell differentiation. They have distinct stages of hematopoiesis that occur in discrete yet functionally analogous sites. Zebrafish myeloid lineages, including monocytes, macrophages, neutrophils and eosinophils, have been reviewed and have been characterized as similar to those in humans<sup>47</sup>. The innate immune roles of these cells offer an efficient defense mechanism during the onset of development. In the case of a viral infection such as influenza, the immune cells are triggered and function accordingly to quarantine the virus by inducing the antiviral state. Macrophages and neutrophils (large, mobile phagocytic cells) can also be recruited to the site of infection to engulf invading species. Macrophages have been known to respond more quickly to infection than neutrophils at about 30hpf<sup>73</sup>. The relatively slower neutrophils respond at about 52hpf to complement activities of the macrophages, partly because the phagocytic capability of neutrophils is relatively low compared to that of macrophages<sup>74</sup>. Precursors of the lymphoid cells (T-cell and B-cells) begin the process of rearrangement and recombination of the genes for immunoglobulin and T cell receptor molecules by day 4. This is the onset of adaptive immune system development. The thymus, which is also a lymphoid organ, produces T cells and B cells for the zebrafish immune system, the pancreas has also been reported to

produce B cells<sup>75,76</sup>. Even though the adaptive immune system begins forming early in zebrafish development, studies have shown that the zebrafish is incapable of mounting a full antibody response until early adulthood, which is about 4 weeks post fertilization. The mode of pathogenic defense up until this point is exclusively dependent on the innate immune system<sup>77</sup>.

In an effort to understand the different maturation states of the immune system during zebrafish development, S.H. Lam *et al* investigated the expression of six immune-related genes of the zebrafish namely: Ikaros, that encodes a transcription factor which is used as an early lymphoid marker; Rag-1 (Recombination activating gene-1), which encodes a protein involved in genomic rearrangement of the T-cell receptor, immunoglobulin loci, and is a suitable marker for maturing lymphocytes; T-cell Receptor Alpha Constant region genes (TCRAC) which encode portions of the antigen receptors of mature T-lymphocytes; three immunoglobulin light chain constant region genes (IgLC) which encode portions of the antigen receptors of mature B lymphocytes. Although there have been cloning and characterization studies on immune-related genes prior to this study<sup>78,79</sup>, there was very little known about the maturation of the zebrafish immune system with regard to its form and function. By employing standard profiling techniques to assess gene expression (quantitative real-time polymerase chain reaction, in situ hybridization (ISH), immuno-affinity purification and Western blotting), Ikaros was detected first, at 1 dpf. The expression thereafter increased gradually to more than two-fold between 28 and 42 dpf before decreasing to less than the initial 1dpf expression level in adult fish (aged 105 dpf). Rag-1 expression levels increased

rapidly (by 10-fold) between 3 and 17 dpf, reaching a maximum between 21 and 28 dpf before decreasing gradually. In adult fish aged 105 dpf however, the expression level of Rag-1 dropped significantly, and was equivalent to the expression level at 3 dpf. T-cell receptor alpha constant region genes and mRNAs of immunoglobulin light chain constant region (IgLC) isotype-1, 2 and 3 were detected at low levels by 3 dpf and their expression levels increased steadily to the adult range between 4 and 6 weeks post-fertilization (wpf). Using tissue-section ISH, Rag-1 expression was detected in head kidney by 2 wpf while IgLC-1, 2 and 3 were detected in the head kidney and the thymus by 3 wpf onwards. Secreted Ig was only detectable using immuno-affinity purification and Western blotting by 4 wpf. A humoral response to T-independent antigen (formalin-killed *Aeromonas hydrophila*) and T-dependent antigen (human gamma globulin) was observed in zebrafish that were immunized at 4 and 6 wpf, respectively, indicating a normal immune response. The findings revealed that the zebrafish immune system is morphologically and functionally mature by 4–6 wpf<sup>77</sup>.

### **1.7 Injection of Zebrafish Embryos**

One of the most common techniques used to introduce materials into zebrafish embryos and larvae is injection. Although invasive, it allows precise targeting of tissues and organs. When conducted under appropriate conditions, such as mild sedation, injections pose minimal risk to zebrafish larvae. During injection, certain substances such as nucleic acids, proteins, or drugs are introduced into the zebrafish, usually at the early stages of development<sup>80</sup>. Injections are typically



conducted with glass needles filled with the material to be delivered. The glass needles can be fabricated easily by carefully drawing out a heated capillary tube with the appropriate inner and outer diameter<sup>81</sup>. The glass needles are then held by a micromanipulator that controls and changes the position of the needle relative to the embryo with high precision. Pressure from compressed air is used to release the content into the embryo or larva.



*Figure 2: A typical micromanipulator for manual injection needle operation in all three axes (x, y and z). It allows for coarse adjustment readings with an accuracy of 100 micrometers. Warner Instruments, Model MM-33, Hamden CT.*

Injection allows rapid delivery of material into the zebrafish. After manipulation of embryos or larvae into a suitable array, an experienced researcher can inject several hundred embryos in one hour, although the relatively high chances of error associated with this technique, can negatively affect the consistency of injection. A detailed injection protocol consisting of zebrafish loading and preparation has been characterized<sup>82</sup>.

### **1.7.1 Standard Techniques**

Injection of zebrafish has been commonplace for decades and numerous procedures have been developed to inject almost every part of the live fish, notably the brain ventricle, the kidney, the swim bladder and the Duct of Cuvier (DC). The DC is a wide blood circulation valley on the yolk sac connecting the heart to the trunk vasculature. Injection through this duct allows quick and efficient systemic infection of zebrafish and is particularly useful for introduction of bacteria into embryos between 1 and 3 dpf. For these injections, the needle is inserted into the starting point of the duct of Cuvier just dorsal to the location where the duct starts broadening over the yolk sac. This location is the deepest section of the duct and therefore provides the lowest risk of puncturing the yolk sac. The injected material will follow the blood flow through the duct of Cuvier, over the yolk sac toward the heart, and can be monitored directly post-injection by monitoring the expanding volume of the duct<sup>83</sup>.

### **1.7.2 Rapid Prototyping and Influence of Technology on Research**

Ranges of technological advancements have paved the way for new and innovative devices and techniques that help make laboratory work more efficient and reliable. The rate of technological advancement has been high within this past decade, which may be attributable in part to the increase in computational power<sup>84</sup>. Another major influence on technological advancement is the emergence of 3D printing technologies for rapid prototyping, which is poised to revolutionize device development in many industries, including healthcare. Since its initial use, additive

prototyping technology has advanced to use in a wide range of applications including tissue engineering, dentistry, construction, automotive and aerospace<sup>85,84,86</sup>. The technology is already changing the way objects are made, with resulting products ranging from tools and toys to clothing and even body parts. 3D printing is part of a process known as additive manufacturing where an object is created by adding material layer by layer, usually at a fraction of the cost and time of standard means such as forging, molding and sculpting. In the medical world, physicians are testing biomaterials for regenerative medicine. Using medical imaging and 3D-modeling technology, surgical teams can now also use 3D printers to create temporary tools that are affixed to the skeletal structure of the patient to provide a precise "blueprint" for reshaping bone structure to perfectly accommodate standard-size implants. Custom-printed drilling guides permit screws to be placed precisely to ensure the best fit with a patient's body<sup>87,88</sup>.

Within the dynamic branch of zebrafish research, prototyping technologies are gradually being introduced to improve the speed and quality of lab work<sup>30,92,97</sup>. These technologies may have the potential to make complex and tedious procedures, such as injection and imaging of chorionated embryos, relatively simple. The following paragraph highlights devices that implement rapid prototyping techniques to make working with zebrafish more efficient.

### **1.7.3 Notable Devices for Zebrafish Injection**

Pardo-Martin et al. at Massachusetts Institute of Technology and Harvard University developed a high-throughput platform for cellular-resolution *in vivo*

pharmaceutical and genetic screens in zebrafish larvae<sup>30</sup>. The automated system is capable of sampling zebrafish larvae and then positioning them for imaging. The system is also capable of manipulating both superficial and deep organs (via femtosecond laser microsurgery). Each cycle of the system includes the following steps: loading, sensing, trapping, injection and flushing. During loading, the system extracts larvae from a reservoir filled with distilled water. A high-speed optical detection system composed of a photodiode and two LEDs detects the entry of larvae into the loading tube. The photodiode senses transmitted and scattered light from the laser light source. By monitoring the light signals, the system can distinguish a larva from air bubbles and debris with 99.99% reliability (n = 100). After loading and detection, the larva moves into a capillary positioned within the angle of view of an optical imaging and manipulation system. Using a fast camera and an automated image-processing algorithm, the larva is coarsely positioned by the syringe pump within focus of the optical imaging system. At the end of one complete cycle, animals can be dispensed back into either individual wells or larger containers by executing the loading process in reverse. While this device boasts of effortless zebrafish manipulation for imaging, it falls short of addressing the tedious process of microinjection: a frequent and necessary step prior to imaging. Design of an entrapment mechanism as part of a sampling device to accommodate an injection needle would add an important manipulation capability.

Rohde *et al* at Massachusetts Institute of Technology developed a high-speed microfluidic sorter with the ability to isolate and immobilize small live animals in a well-defined geometry (within a chip) for screening phenotypic features in

physiologically active animals. The integrated chip contains individually addressable chambers that can be used for incubation and exposure of individual animals to biological compounds and high resolution imaging without the need for anesthesia. Besides its sorting and immobilizing function, the channels within the microfluidic chip can be combined in various configurations to permit a multitude of complex functions such as small animal incubation (eg. *C. elegans*), immobilization and independent subcellular resolution imaging<sup>89</sup>. This system is versatile but shares a similar limitation with the system made by *Pardo-Martin*<sup>30</sup> and his team: it does not address the upstream procedure of animal injection. Furthermore, the high multifunctional capabilities of this system might make it susceptible to cross-contamination during use. Both the mechanical and electrical complexity of the system also raises durability concerns.

Bischel *et al* at University of Wisconsin-Madison designed a zebrafish entrapment device that can be used to quickly and repeatedly position zebrafish embryos in a predictable array with the help of a pipette. The Zebrafish Entrapment by Restriction Array (ZEBRA) is well suited for use with automated microscope stages, thereby reducing the amount of imaging time and further increasing throughput compared to traditional methods. ZEBRA was designed and optimized to immobilize 3–5 dpf zebrafish embryos in a predictable array without the use of agarose. The device consists of an enclosed channel with a restriction width that is accessed through an input and an output port<sup>90</sup>. For normal function, ZEBRA must be filled with water (this process requires oxygen-plasma treatment to render the inside of the channels hydrophilic). After initial filling, a pipette can be used to add a

droplet of water containing a selected zebrafish embryo to the input port of the device. The main function of the device is governed by passive pumping: a phenomenon by which surface tension induces pressure differences to drive fluid movement in closed channels<sup>91</sup>. As a result, water is driven from the smaller input port (with higher surface tension) to the larger output port (with lower surface tension). The zebrafish is then trapped in place upon reaching the channel restriction. Users can choose whether to load the zebrafish into the device headfirst or tail-first depending on the desired application. Passive pumping works reproducibly as long as there is a closed channel between an inlet and an outlet<sup>91</sup>. This makes the device more practical and portable since it is not dependent on a power source. Despite its inherent advantages, the device does not accommodate zebrafish injection. The flow rate and aspiration conditions within the channels appear to be dependent on the size of the droplet placed at the inlet of the device. As the droplet collapses, the aspiration rate decreases thus creating a device constraint that can potentially limit the length of the channel between the inlet and the outlet ports<sup>91</sup>. Although less energy-efficient, employing active pumping in this scenario can potentially eliminate this constraint to permit longer channels that can accommodate zebrafish, as well as other animals, such as *C. elegans*.

Westhoff *et al* at University of Heidelberg formed a piece of brass to serve as a negative mold to cast agarose to yield a series of wells capable of holding zebrafish for imaging and micromanipulation<sup>92</sup>. The brass mold casts indentations into an agarose gel by inserting the tips of the mold into unset agar solution and allowing the solution to gel. The mold is removed, leaving voids that are contoured to hold

zebrafish larvae for imaging. While this device requires significant manual interfacing, it minimizes the issue of having to insert and orient specimens in an agar medium. Users simply pipette their specimen into the wells prior to imaging. Evenly spaced wells allow screening of large numbers of specimens and can be automated with a translation stage. While the device offers a simple way for users to probe and organize large quantities of specimens, it leaves little room for automation of trans-locating fish into the device. As a result, more user interaction is needed to move and organize the specimens. Automating this process would allow for minimal user interaction between the user and the device.

The devices discussed above all demonstrate innovative approaches to eliminating common problems of working with zebrafish, such as manipulation; however, none of them is applicable to the principal function of zebrafish injection. Using the zebrafish as an animal model for IAV studies involves systematically and reliably introducing the virus into individual larvae via injection. A device to conduct and immobilize zebrafish specimens for injection will be invaluable to IAV studies, particularly where sample sizes are very large. This project has been directed toward design and fabrication of an automated device that will help solve this problem. The main goal of the proposed device is to provide a means for storing and gently conducting zebrafish from a reservoir to a chamber for immobilization and injection. This will minimize direct interaction between the user and specimen, with the goal of reducing injection/handling time in experiments and to maximize reliability and laboratory efficiency, as well as to minimize long-term costs.

## CHAPTER 2

### METHODS

#### 2.1 Overview

The device employs a system to conduct 48-72 hour old zebrafish through a liquid medium (egg water) using a syringe pump. The complete system consists of three main subsystems namely the pump, optical detection and entrapment components. The device works by aspirating individual fish through a tube via a pressure gradient created with a syringe pump. Each cycle of the device involves the following steps: (1) loading, (2) sensing, (3) trapping, (4) injection and (5) flushing. During loading, a single larva is extracted from the reservoir and conducted through a tube past the optical detection subsystem. At the sensing stage, the optical detection subsystem composed of a photodiode and a laser, senses transmitted light from the laser and discerns the entry of larva from air bubbles and debris with precision. Upon larva recognition, the specimen is then conducted to the entrapment dock (step 3) where it will be immobilized for injection (step 4). The final step (5) involves conducting the larva out of the entrapment dock and subsequently out of entire system for further analysis. The syringe pump is pre-programmed and manipulated with LabView, the control software. This device will primarily serve IAV researchers who intend to introduce vaccines, pathogens and other experimental materials into many individual zebrafish larvae.



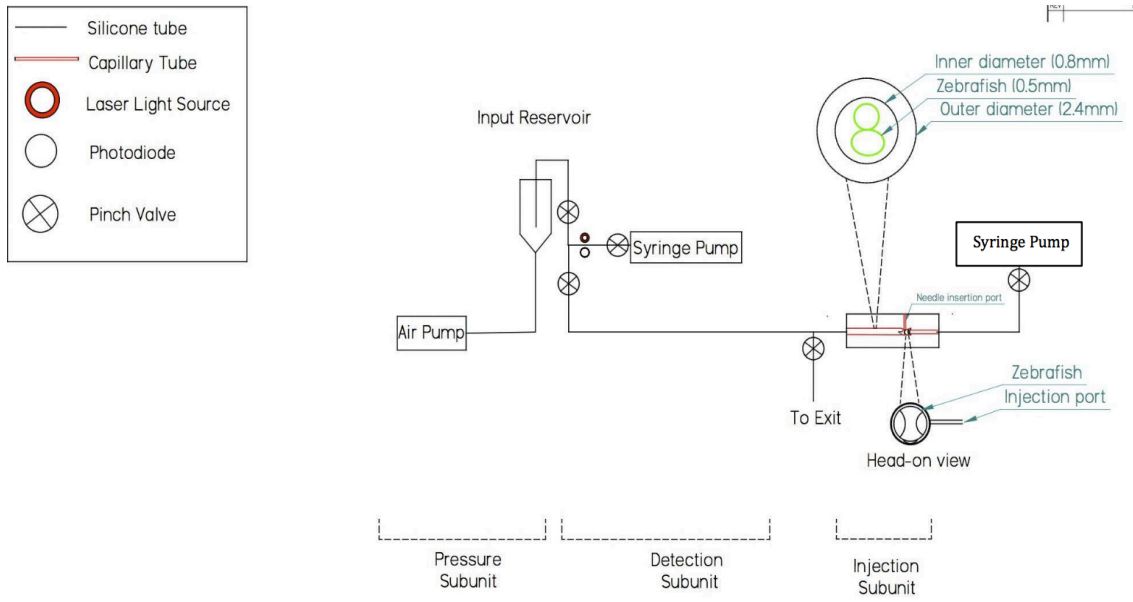


*Figure 3: Device schematic and design. The device offers minimal interaction and seamless aspiration of zebrafish specimen, ultimately trapping and immobilizing it for microinjection of biomaterials.*

The following sections describe in detail the design and construction of the device components.

## 2.2 Pump Subunit Components

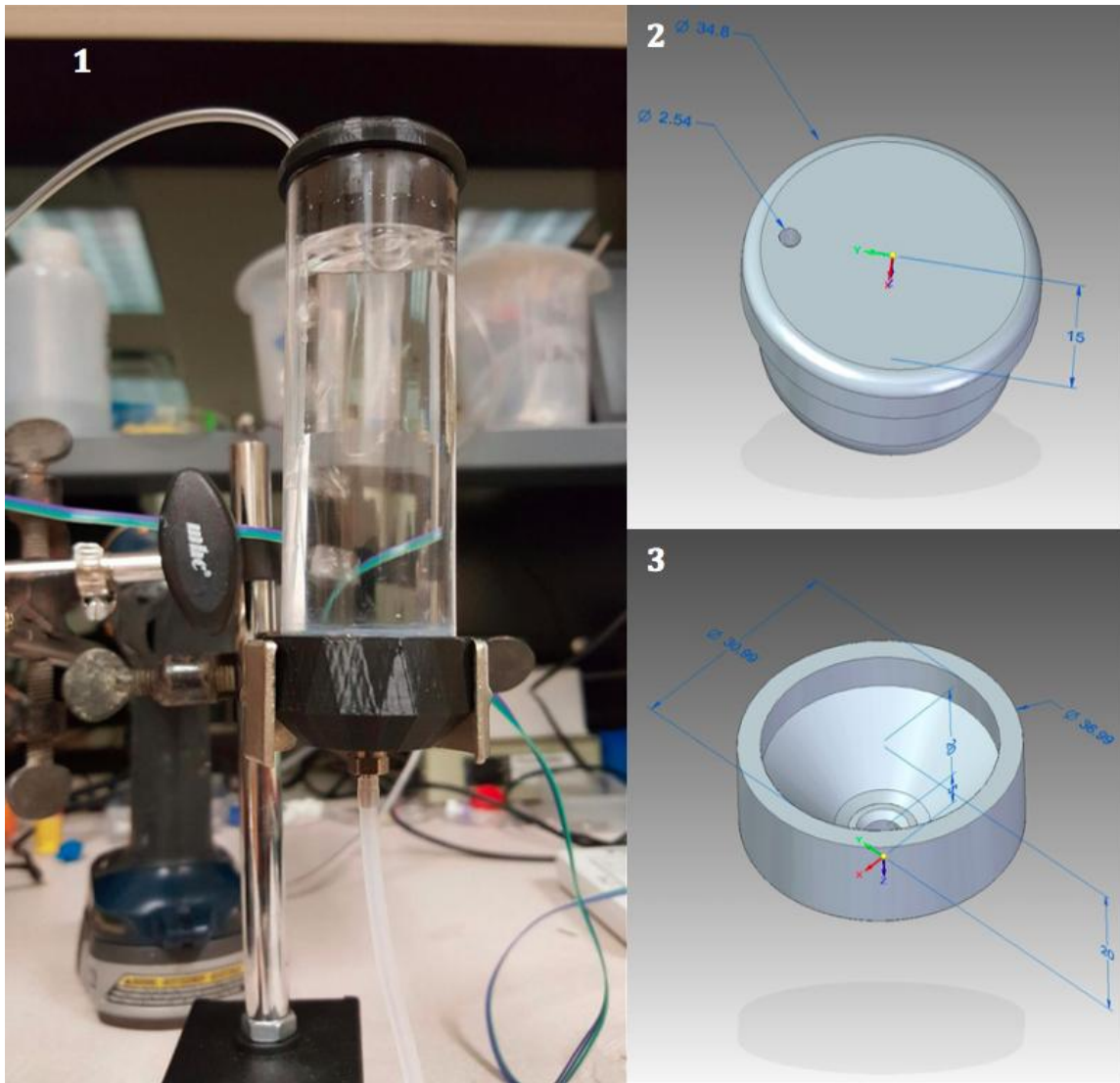


*Figure 4: An image of the input reservoir. The assembled reservoir is shown in Figure 4.1; Figure 4.2 and Figure 4.3 show the design renderings of the top and bottom reservoir caps, respectively.*

The device pictured above serves as the entry point of the zebrafish specimen into the device. With a maximum internal volume of 60mL, the reservoir is capable of accommodating about 50 individual 48-72 hpf larvae. When filled with egg water (*Figure 4.1*), the unique shape and design allows enough room for the fish to swim and eventually be removed by suction through the outlet tube positioned along the wall of the reservoir's bottom cap. During testing, it was observed that the zebrafish larvae had the tendency to sink downward, toward the deepest part of the bottom cap. This made it difficult for specimen to be randomly removed from the reservoir through the tube, thus dramatically reducing the larvae output rate. To remedy the problem, a bubbler was introduced. A narrow hole was drilled through the deepest part of the bottom cap to allow for a silicone tube to be threaded through and connected to the bubbler. An Aqua Culture single outlet aquarium air pump was used as the air source *Figure 5*. It includes a check valve that prevents the siphoning of reservoir water into the air pump in the event of a power loss.



*Figure 5: Aqua Culture single outlet aquarium air pump. The pump is originally an air pump designed for a 5- to 15-gallon aquarium. It includes a check valve (blue valve pictured) that can help prevent the siphoning of reservoir water into the air pump in the event of a power loss.*

Pressure is provided to the system with a New Era NE-1000X Bidirectional Syringe Pump. The pump supplies negative pressure (withdraw mode) for a brief period to cause specimen to be withdrawn from the reservoir and into the system where it will be sensed by the laser diode/photodiode photodetection system. The pump then switches to positive pressure (infuse mode) to allow the specimen to advance through the system.



*Figure 6: New Era NE-1000X bidirectional programmable syringe pump. With fully programmable and stand-alone capabilities, the pump can be programmed for up to 41 pumping phases that change pumping rates, set dispensing volumes, insert pauses, control and respond to external signals. It has a dispensing accuracy of  $\pm 1\%$ .*

### **2.3 Optical Detection Subunit Components**

The optical detection unit helps with the direction of travel of specimen within the system by sensing the presence of zebrafish, which prompts the syringe pump to switch between supplying positive and negative pressure. The two main elements used for sensing are: a 5mm transparent cylinder head photodiode (PD)

(LLS05-A, Senba Optical Electrical Co., Ltd) and a 4.5V 650 nm red laser diode module (#01444878, LightInTheBox Co., Ltd). During normal operation, the red laser beam is focused onto the photodiode and a base (unobstructed) voltage reading is observed and recorded (voltage comparator circuit yields a HIGH signal). The movement of specimen past the light beam reduces the voltage reading, resulting in the voltage comparator circuit producing a LOW signal, indicating the presence of a larva as depicted in the cartoon (*Figure 7.1*).

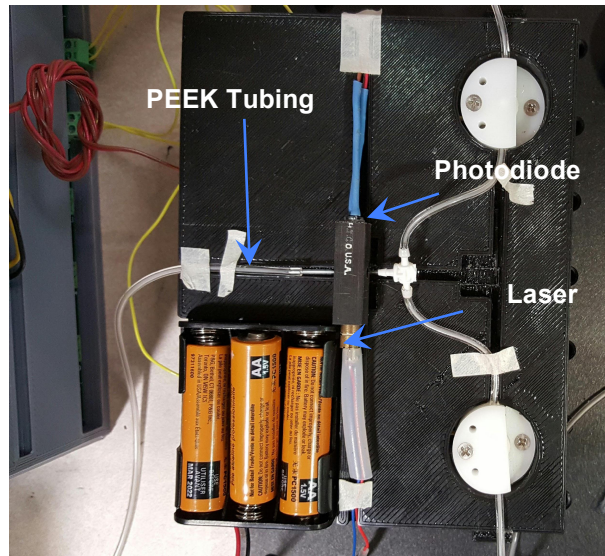
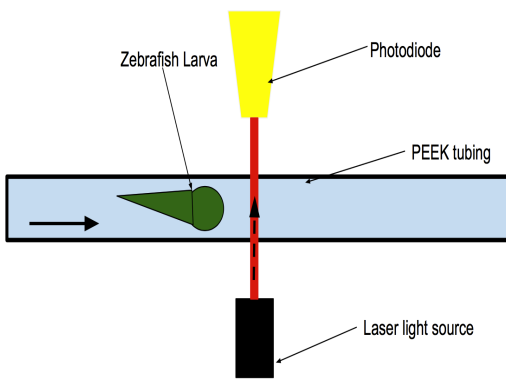


*Figure 7: An image of the optical detection unit components. Figure 7.1 depicts a cartoon that highlights a zebrafish larva moving past the red laser beam to indicate the presence of a specimen; the blue selection within Figure 7.2 shows the actual setup of the detection system mounted on a 3D printed harness.*

## 2.4 Entrapment Dock

A critical component of the injection system is the entrapment dock, a device that immobilizes the specimen for injection. The dock was designed using SolidEdge rapid-prototyping software and 3D printed using a transparent photopolymer that

provides a suitable level of surface smoothness. The polymer (VeroClear-RGD810) is a rigid, nearly colorless material with dimensional stability for general purpose, fine-detail model building and visual simulation of transparent thermoplastics. The entrapment dock dimensions are represented in *Figure 8*.

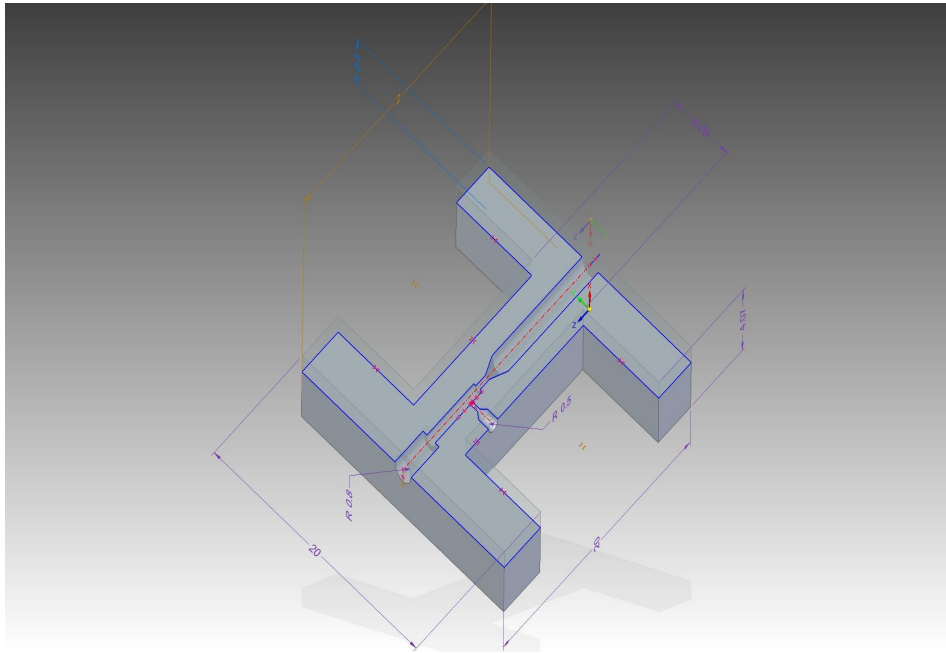


*Figure 8: Image of the entrapment dock with highlighted channels and dimensions in millimeters.*

The channels within the dock are designed to accommodate the shape of a 2-day old zebrafish larva. Beginning from one end of the dock, the channel begins with a *1mm* diameter opening to accommodate the capillary tube from the automated delivery system. It then narrows to a micro-constriction that is small enough to allow some excess water to flow past the specimen to the other end of the dock while simultaneously trapping and immobilizing the specimen for injection. An

opening perpendicular to the trapped specimen serves as an entry for the injection needle.

Despite the convenience and practicality of 3D printing, the ability to fabricate small, intricate designs such as microchannels can sometimes be limited. Although printers and techniques exist for micro fabrication, the cost of securing a high-resolution printing unit is high, with prices starting at 20,000 USD. Less expensive units can perform similar functions to the more expensive machines, but with less precision. The lab in which the entrapment dock was printed (Innovative Media Research & Commercialization Center, University of Maine) was equipped with an intermediate resolution 3D printer (Stratasys Objet30, SUP 705 support material), and so several challenges influenced the final design of the port. Most notable amongst these was the problem of lodged support material within the microchannels. Most 3D printers employ the Additive Manufacturing (AM) design technique where successive layers of material are formed under computer control to create an object; it is analogous to building a brick wall layer by layer. If a particular design is supposed to have an enclosed opening or channel, support material is deposited into the cavities to hold up the structure as the rest of the object is being built. As a result of this process, all of the entrapment docks were filled with support material and post-printing procedures to remove it proved futile. Some of the procedures used were: applying mild heat, using biodegradable solvents and manual excavation of the material using a thin syringe needle. These problems spawned the idea of bisecting the original design of the port horizontally and printing both pieces independently, as displayed in *Figure 9.2*. This exposes the

channels and allows for easy removal of the support material without damaging the integrity of the channels. A supporting harness was later designed and 3D printed to rejoin and clamp together the pieces of entrapment dock *Figure 9.3*.



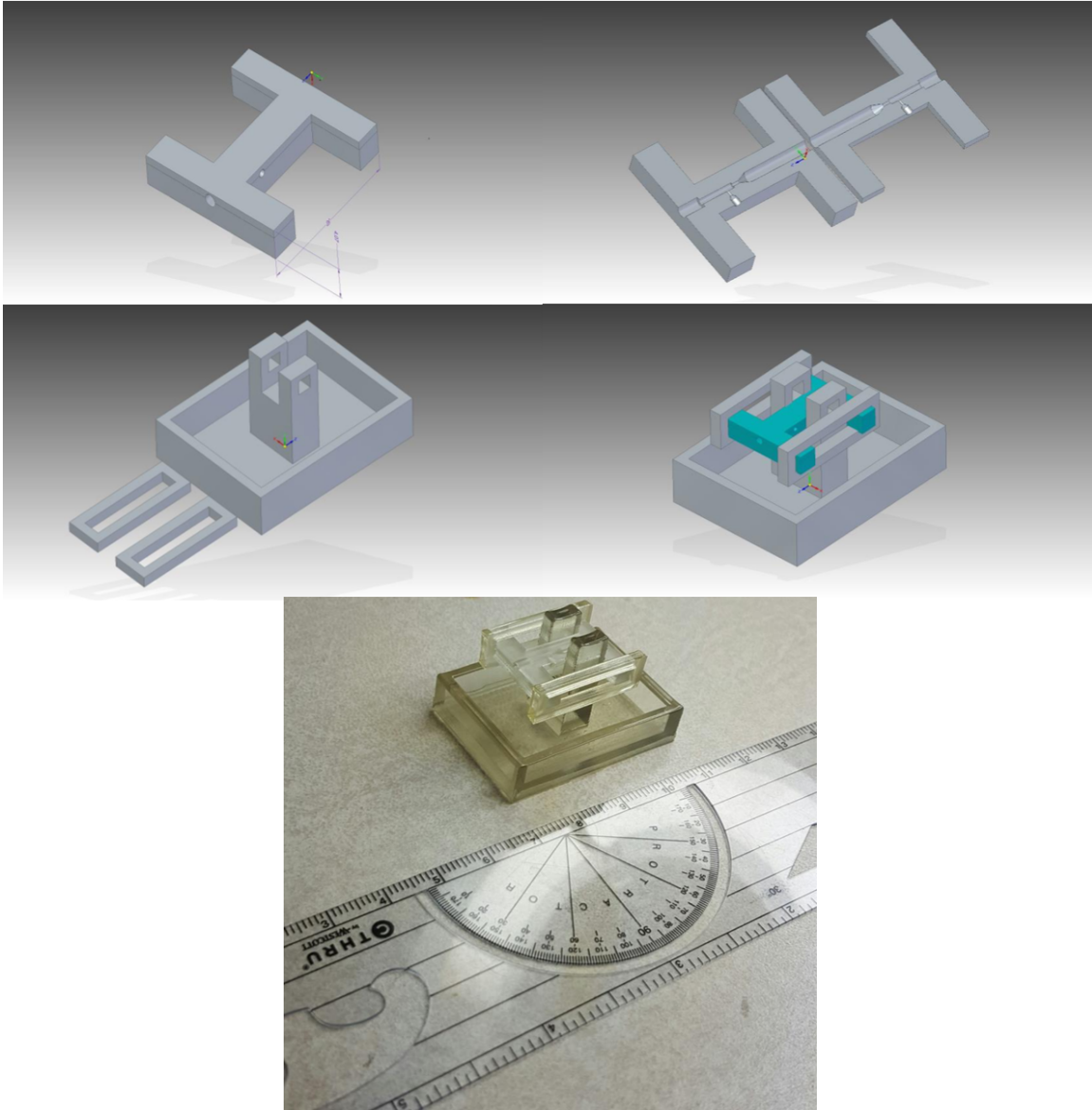


*Figure 9: Images of the entrapment dock and its supporting components designed using Solid Edge CAD software. The 3D printed solid is a transparent material (VeroClear-RGD810) that provides dimensional stability and a rigid finish. Figure 9.1 is an image of the assembled entrapment dock; Figure 9.2 depicts the two split-pieces of the entrapment dock; Figure 9.3 shows the rendering of the supporting harness that clamps and keeps the split-pieces in place; Figure 9.4 shows the rendering of the completely assembled device with the entrapment dock highlighted in green; Figure 9.5 is an image of the completely assembled device.*

### 2.4.1 Biocompatibility

3D printing and photopolymer composition have improved tremendously within the past few years, and problems with biocompatibility have mostly been overcome by post-processing the 3D printed device and optimizing the chemistry of the resins used to create micro- and milli-fluidic platforms. The polymer used to print the entrapment dock (VeroClear-RGD810) is dimensionally stable and is approved for medical applications<sup>93</sup>. In future pursuits to perfect the entrapment dock and to accommodate different organisms, an advanced polymer (MED610, made by Stratasys) could be used. This plastic has a wider biocompatibility range and might serve as a better alternative<sup>94</sup>.

*Macdonald et.al* at the University of Glasgow assessed the biocompatibility of four commercially available 3D printing polymers (VisiJetCrystal EX200, Watershed 11122XC, Fototec SLA 7150 Clear and ABSplus P-430) with zebrafish and observed the key developmental markers in the developing embryos. Their results showed that the four photopolymers were very toxic to the embryos, resulting in fatality in most cases<sup>95</sup>. These results re-emphasize the importance of using biocompatible materials to achieve reliable results, especially when conducting experiments in which morphological changes are analyzed. It is becoming widely acknowledged that more detailed biocompatibility testing must be provided by manufacturers before 3D printed objects are used in different biosystems<sup>96,97</sup>.

## 2.5 Specifications and Parameters

1. The 48-72 hpf zebrafish larvae can be aspirated up to a maximum flow rate of  $330\text{mm}^3\text{ s}^{-1}$ , given tubing dimensions of 0.8mm inner diameter x 2.4mm outer diameter.
2. The maximum speed the larvae can attain in this tubing without deformation is  $656\text{mm s}^{-1}$
3. In this system,  $\text{Re}=528$  at  $20^\circ\text{C}$ .
4. The maximum aspiration rate at the delivery tube/capillary junction should be below  $83\mu\text{L s}^{-1}$  to avoid damaging the larvae.
5. The inner diameter of the input capillary is  $800\mu\text{m}$

## 2.6 Electronics

To automate movement of the larvae in the present system, electronic sensors (e.g. photodiode) and actuators (e.g. syringe pump), were used to control fish movement through a LabVIEW interface. The myDAQ (National Instruments, Austin, TX) was used to detect events and to control devices, such as the SC5 solenoid controller (RW Automations, *Figure 10*) used to control the solenoid valves.

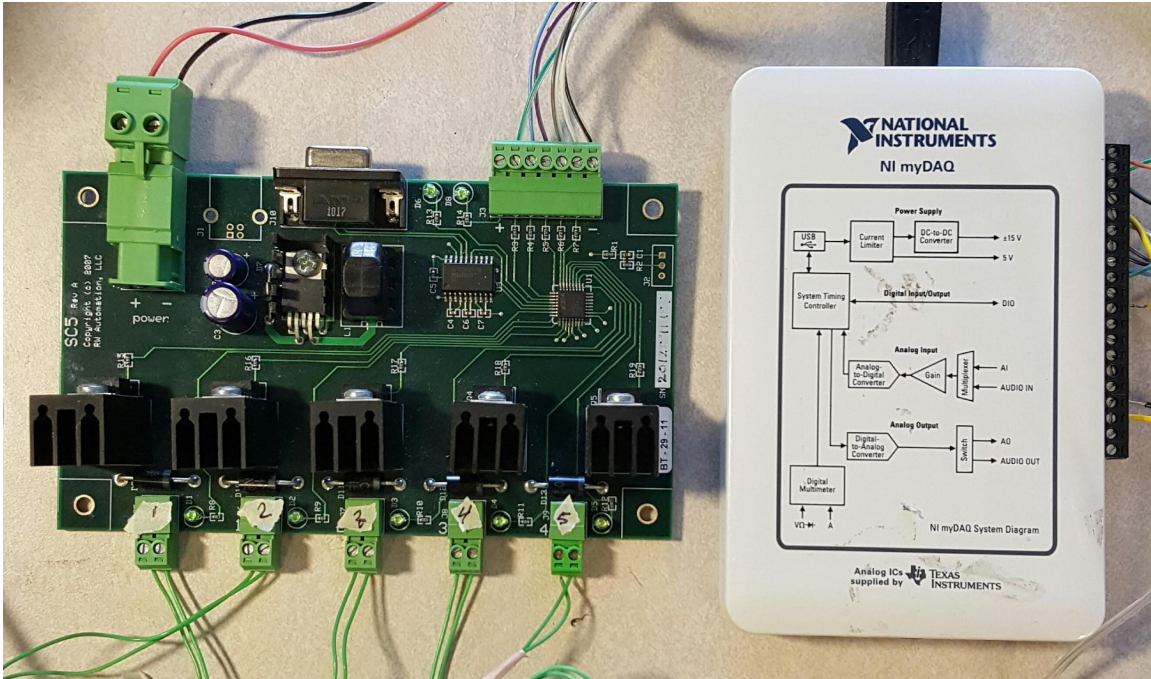
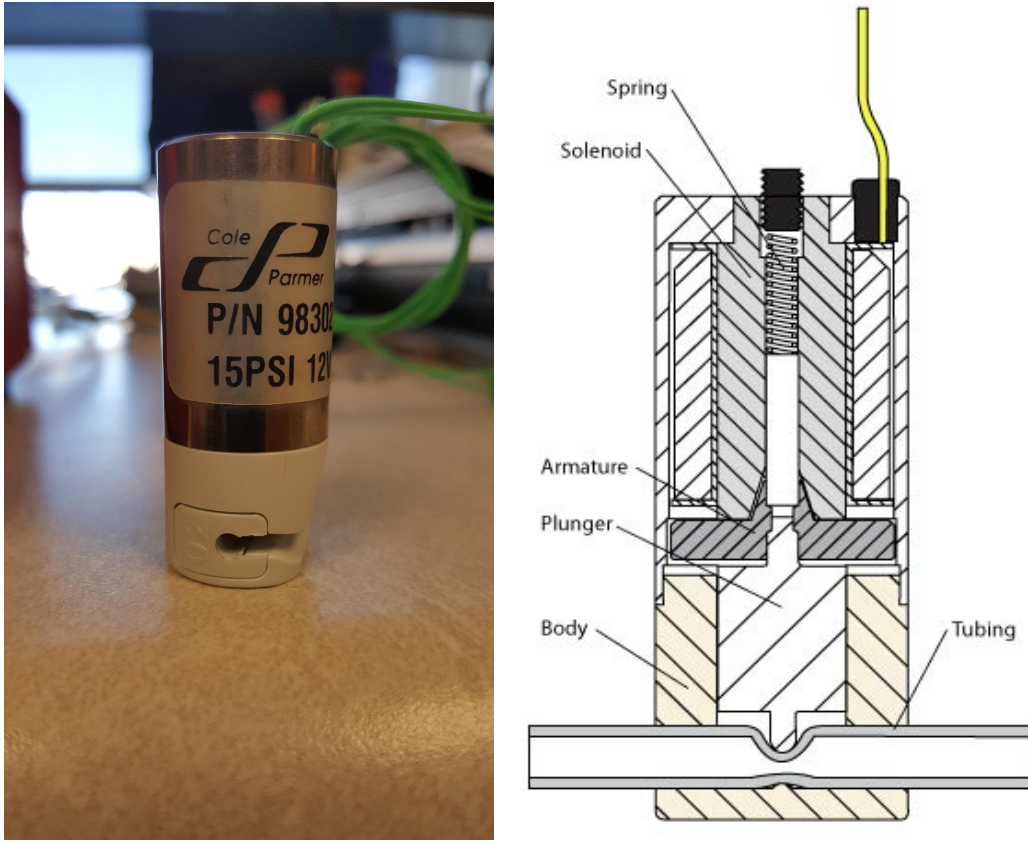


Figure 10: Electronic Components. RW Automation SC5 Solenoid Controller board equipped with power, communication, and status LEDs (Left); National Instruments myDAQ (Right)

The myDAQ from National Instruments (NI) is a Data Acquisition (DAQ) unit that interfaces with the graphical programming software package, LabView, and allows for simple external control of connected devices. NI myDAQ is a simple and intuitive DAQ device with analog inputs, analog outputs, digital inputs and digital outputs. The digital output channels are used to control the Transistor-Transistor Logic commands (TTL) that trigger the solenoid pinch valves. The myDAQ was also be used as a power supply.

The RW Automation SC5 solenoid controller permitted programmable control of the solenoid pinch valve depicted in *Figure 11*. The board controls five independent valves by utilizing a peak-and-hold algorithm. This allows the user to

energize each solenoid valve at its full rated voltage for fast actuation and strong pull. The SC5 then automatically reduces the average voltage applied to the solenoid to conserve power and prevent overheating of the solenoid in the open/on position.



*Figure 11: Cole-Parmer two-way normally closed solenoid pinch valve. 12 VDC, 1/16" ID x 1/8" OD tubing. The solenoid controlled pinch valve clamps with a force of 15 PSI with a 25 msec response time.*

When triggered, the solenoid controller applies 12V to the solenoid valves for 0.5 sec, then reduces the voltage to a holding level of ~4.5V. This minimizes overheating of the solenoid. The SC5 controller is under TTL control and opens or closes the solenoid pinch valves with high or low voltage signals from the DIO

channels of the myDAQ controller. Low to high voltage TTL input transitions trigger the solenoid valve opening, while high to low TTL voltage transitions turn off the solenoid voltage to disable the solenoid and close the valve (NC state). TTL inputs of the solenoid controller board are interfaced with DIO ports 0-4 on the myDAQ and controlled by a LabView VI with Boolean controls.

To enhance the clarity of data and to permit higher data acquisition rates from the optical detection system, a precision high-speed voltage comparator was used (Texas Instruments LM 339N) to convert the photodiode voltage output to a TTL signal. The voltage comparator functions by comparing the differential voltage between the positive pin (sporadic voltage from PD) and negative pin (stable predetermined voltage from myDAQ), then generating a TTL signal based on the input differential polarity *Figure 12.1*. This circuit renders the system less sensitive to potential false readings from the PD.

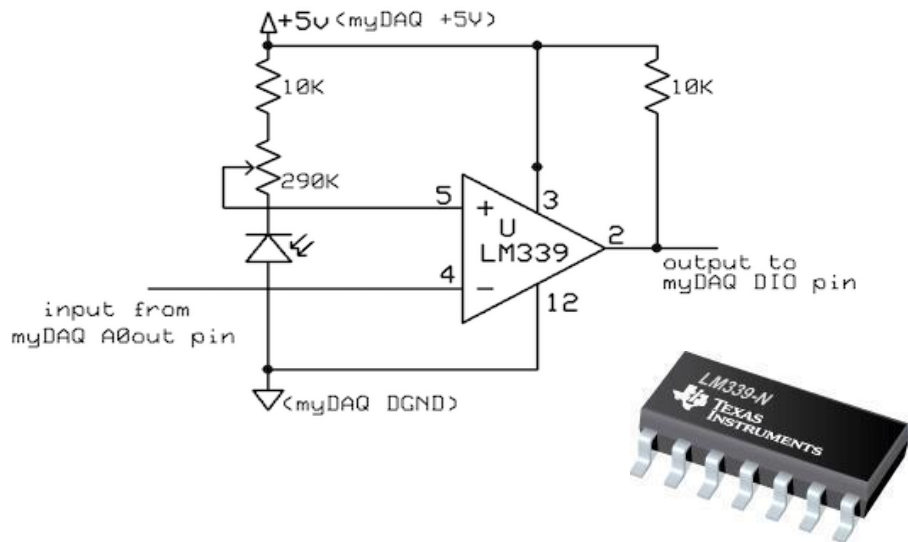


Figure 12: Image of the functional circuit diagram. Voltage comparator (left); wiring of comparator on a breadboard (Right)

The LM339N series IC consists of four independent precision voltage comparators with an offset voltage specification as low as 2 mV maximum for all four comparators. The comparator is devised to operate from a single power supply over a wide range of voltages and to directly interface with TTL (Transistor-Transistor Logic) and CMOS (Complementary Metal-Oxide-Semiconductor).

### 2.6.1 Control Maps/Software Programming

Most of the system is managed manually through a virtual instrument dashboard designed in LabView, *Figure 13*. The platform allows automation of the solenoid valves and the syringe pump to aspirate zebrafish larvae into the entrapment dock.

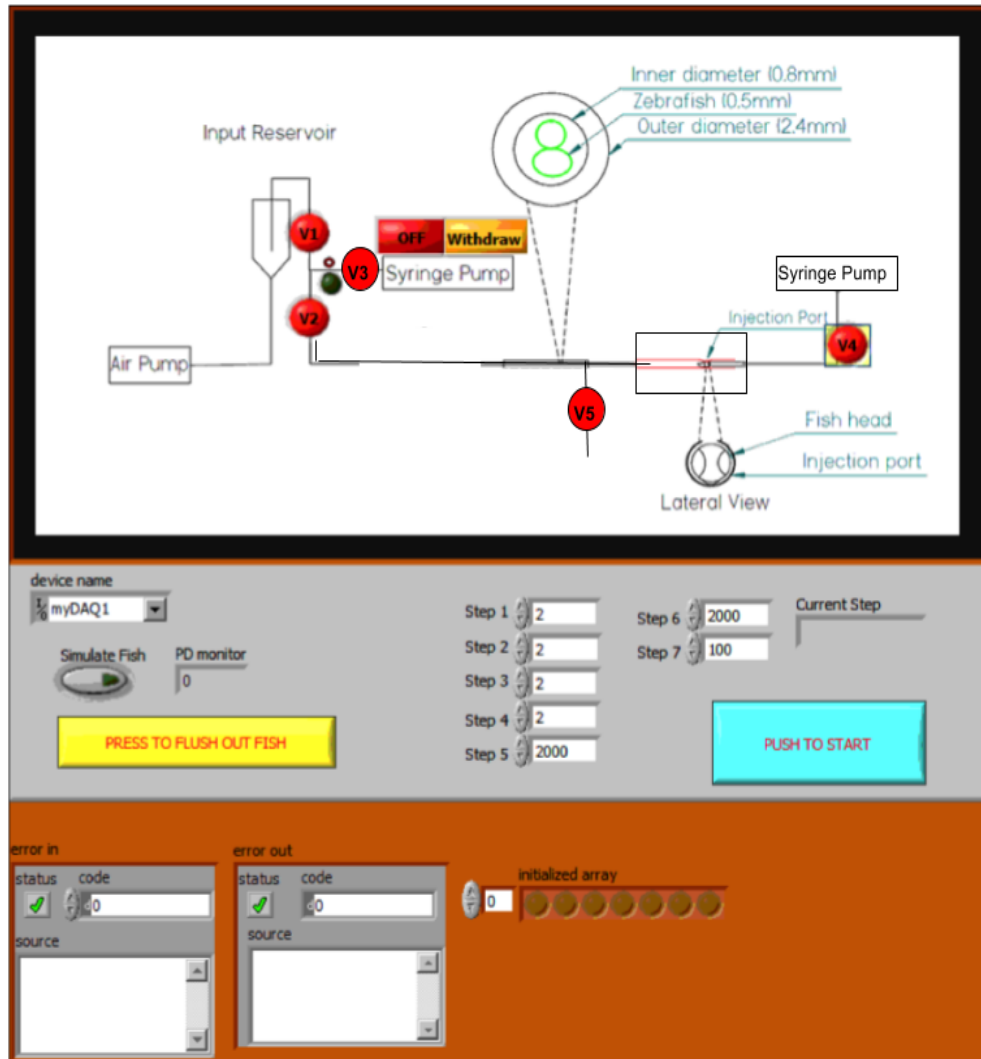


Figure 13: LabVIEW control dashboard. It controls the automation parameters such as the duration of injection; solenoid on/off commands and syringe pump functions (pump/withdraw).



## LabView Test Setup Routine

The following is the data flow diagram for the LabView routine, which controls the coordinated functions of the syringe pump, the pinch valves and the optical detection system.

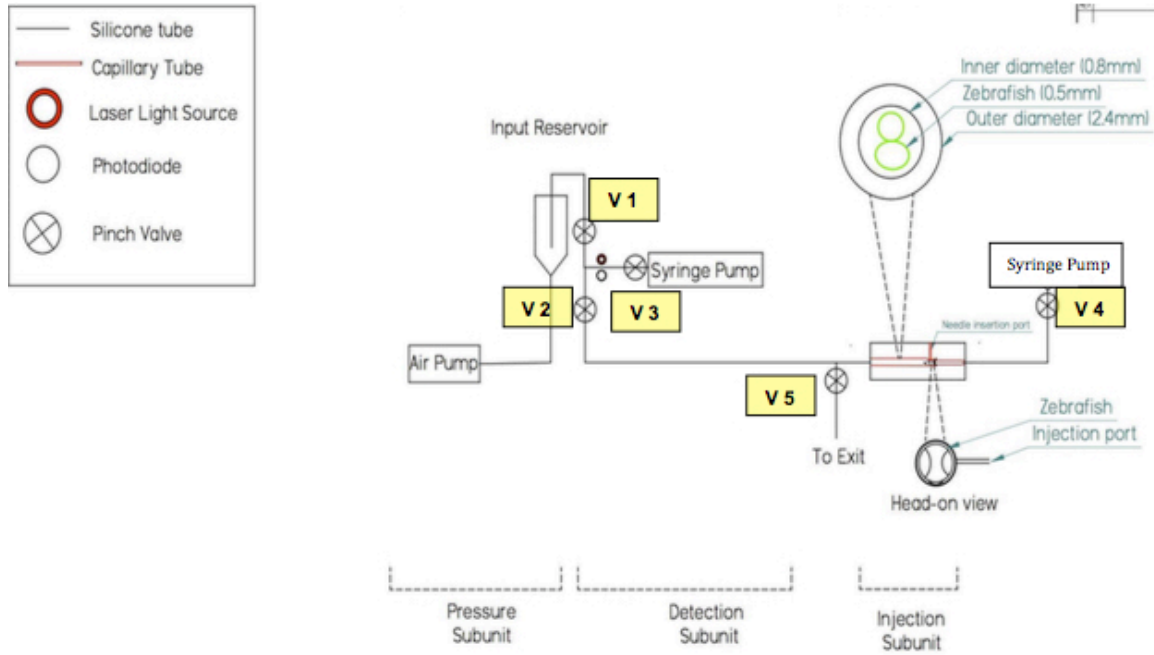


Figure 14: Valve/syringe pump control map

All the solenoid valves are normally closed. A cycle begins with the opening of valve 1 and valve 3. The syringe pump starts withdrawing at a given flow rate until a larva is picked up from reservoir 1, conducted through the tube and detected by the optical detection system. The syringe pump immediately stops withdrawing and valve 1 and valve 3 close. Next, valve 2 and valve 3 open, followed by the syringe pump, in infuse mode, aspirating the larva at the set flow rate to the entrapment dock. Valve 2 closes to prevent backflow. Injection takes place. Valve 4

and valve 5 open after injection. Syringe pump 2, in infuse mode, flushes the larva out of the entire system.

The detailed setup and program commands are highlighted in the appendix.

## CHAPTER 3

### EXPERIMENTAL RESULTS AND DISCUSSION

#### 3.1 Input Reservoir Efficacy Test

To evaluate the specimen output rate of the reservoir, a system test was conducted.

##### 3.1.1 Procedure

The reservoir was filled to capacity (60mL) with egg water (60 $\mu$ g/mL) at room temperature (21°C), *Figure 4.1*. The bubbler was then turned on to prevent settling, thereby increasing the likelihood of larva uptake into the system. 50 individual zebrafish larvae were then introduced into the reservoir. The zebrafish were anesthetized with a 200 $\mu$ g/mL solution of tricaine before use. With the larvae floating freely within the reservoir, the aspiration tube was lowered into the chamber and the syringe pump was set to withdraw mode at the following flow rates for 60 seconds: 10mL/min, 8mL/min, 6mL/min and 4mL/min. The number of larvae aspirated from the reservoir was then recorded and the entire procedure was repeated 10 times, consecutively.

##### 3.1.2 Results

For the entrapment system to be more efficient than the traditional injection method, the reservoir should expel the larvae from the system at a base rate of 3 fish per minute. The test of the reservoir at the highest flow rate (10mL/min) generated an average output of about 6 larvae per minute *Figure 15*. This translates to 1 larva

output every 10 seconds, which is a relatively shorter duration than the remaining time it takes a larva to complete the rest of the cycle. This implies that the reservoir must have an output rate high enough to support the entire system. In spite of the high output rate, only one larva can be processed by the system for any given cycle. The high output rate of the reservoir suggests that it has the capacity to feed multiple entrapment systems simultaneously.

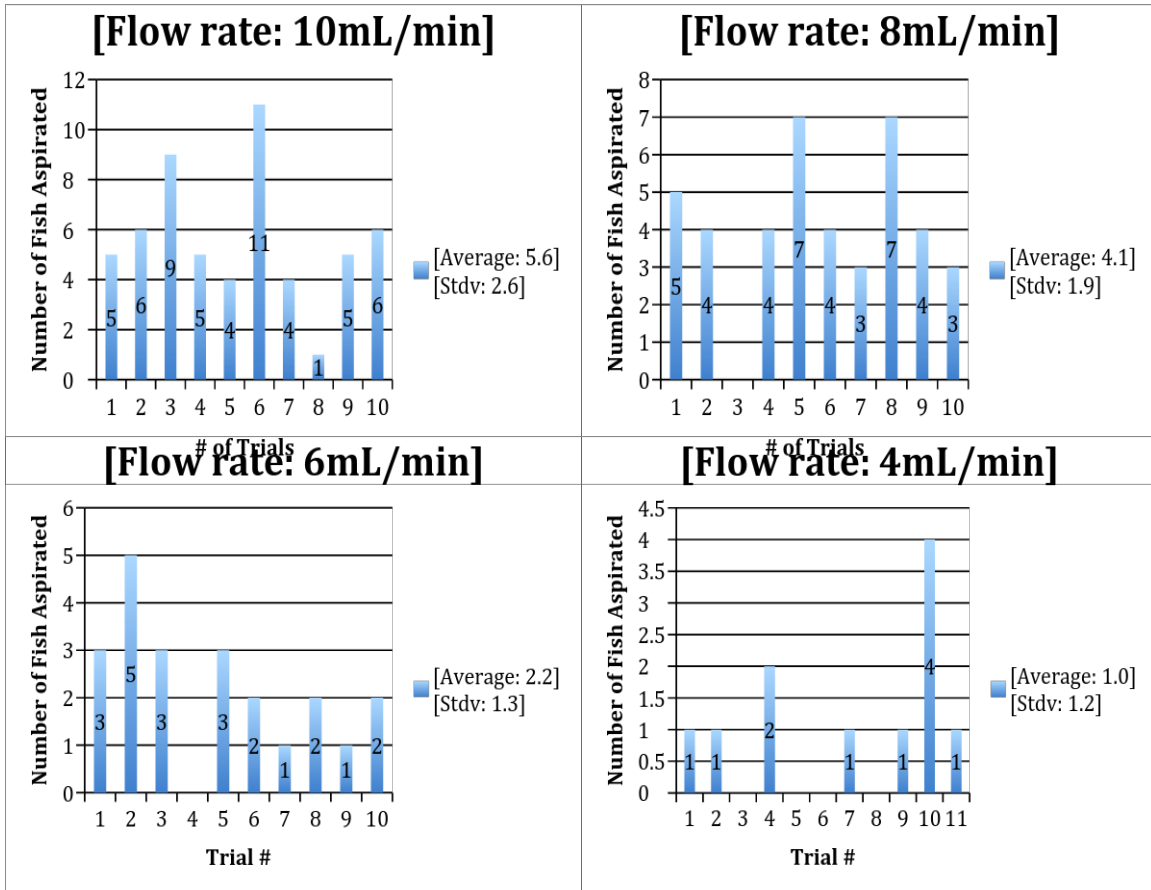


Figure 15: A bar graph depicting the number of zebrafish larvae collected after 60 sec at different flow rates.

### 3.2 Optical Detection Unit Efficacy Test

To evaluate the sensitivity of the optical detection unit, a system test was conducted routinely.

#### 3.2.1 Procedure

First, the 650nm laser module was powered on, with majority of the light beam centered on the photodiode (PD). At this point the LabView software, registered a basal high TTL signal (1,TRUE). Ten individual zebrafish larvae (~48hpf) were then fed through the tube, past the laser/PD, at 10 mL/min. The

decrease in light detected by the PD resulted in a low TTL signal (0,FALSE) from the comparator as the larva passed between the laser and the photodiode and was monitored by the control software.

### **3.2.2 Results**

The results from sensor tests proved that the light detection system effectively detected larvae. The waveform graph, *Figure 16*, displays 10 individual peaks that correspond to the 10-zebrafish specimens used in this test. The initial voltage reading (without a comparator circuit) from 7-14 seconds indicates the observed voltage before water or zebrafish larvae were introduced into the tube. The background noise apparent in several positions on the chart (ex. 14-25 seconds) can be attributed to air bubbles. The control software traces the recorded voltage readings that registered below the basal reading (tube+water+specimen), thus allowing us to discern background noise from useful data.

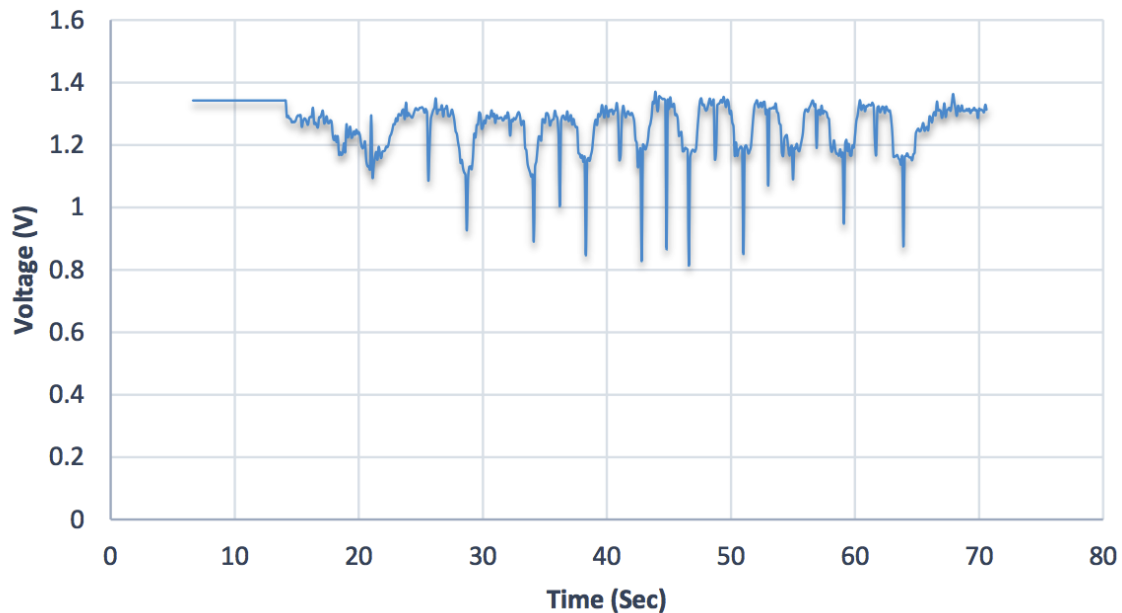


*Figure 16: A waveform chart of the photodiode voltage spikes with respect to time. The base reading from the PD is 1V. The rest of the labeled peaks registering sub-basal voltages indicate the presence of a zebrafish specimen. The comparator circuit was not used to condition these raw voltage signals.*

### **3.3 Entrapment Dock Tests**

The entrapment dock is the main part of the system with the core function of immobilizing 48-72hpf zebrafish to allow tail injection. A series of test trials were conducted to assess its ability to entrap and immobilize 48-72hpf zebrafish.

#### **3.3.1 Procedure**

To test its ability to accomplish trapping, individual 72hpf zebrafish were introduced into the dock via the inlet channel and subsequently flushed out. For every trial that was conducted (n=100), the larva was successfully immobilized regardless of orientation (head/tail entry) as illustrated in *Figure 17*.

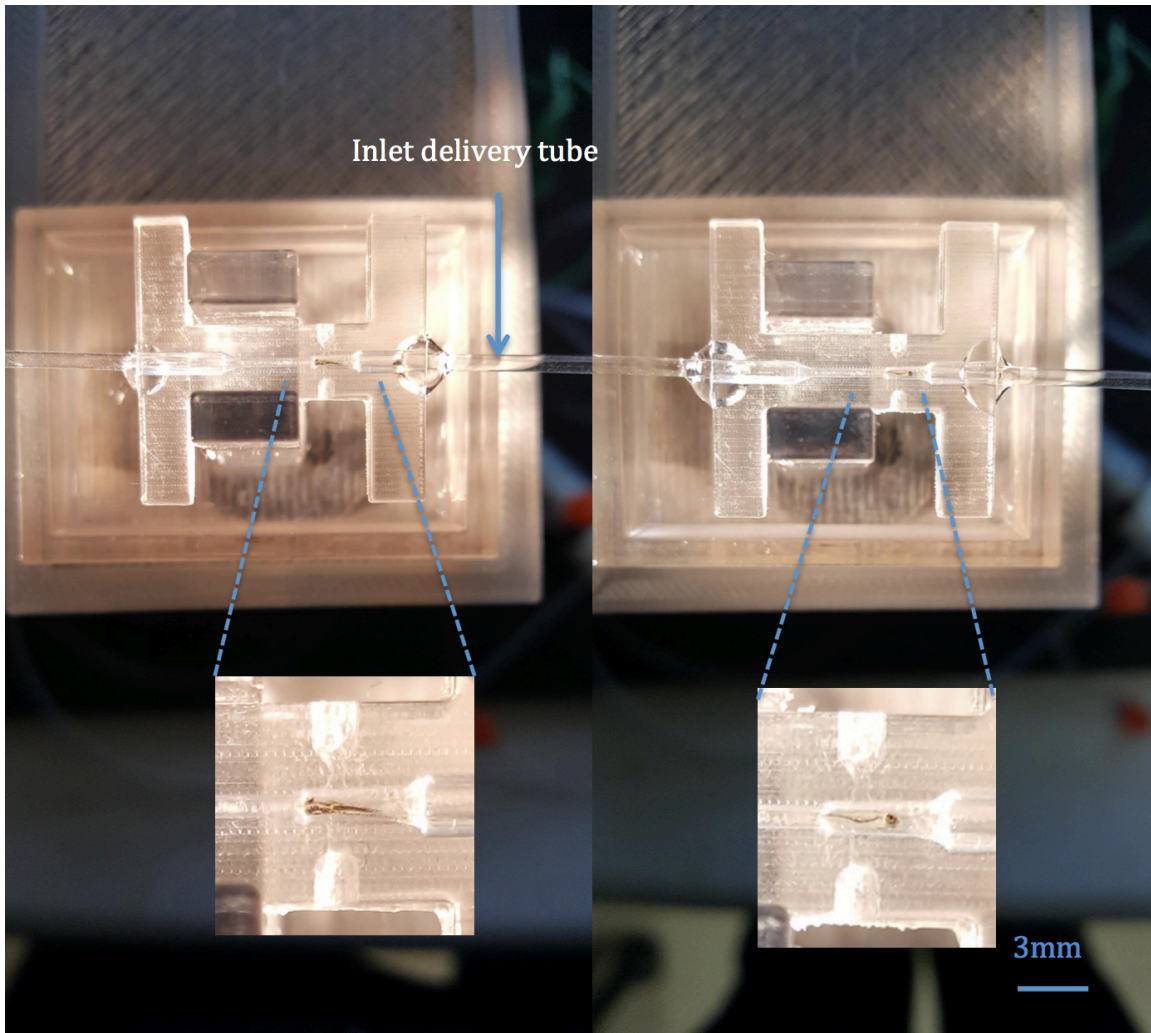


*Figure 17: Image of the entrapment dock illustrating the immobilized zebrafish larvae in the two possible orientations. Head-on arrival (left image) and tail arrival (right image)*

### **3.4 Average Duration of Screening Steps (1 Cycle)**

The overall duration for one cycle through the system was determined in this test.

#### **3.4.1 Procedure**

By timing each automated stage of the processes (loading, trapping, injection and flushing) within one cycle, the average cycle time was calculated. Since the flow rate is varied at certain stages within a given cycle, timing each step provides a more



accurate projection of the overall duration of one cycle.

Step	Flow Rate (mL/min)	Time (sec)
Reservoir → PD	10mL/min	9±6.5
Reservoir → PD	8.0mL/min	10±10.4
Reservoir → PD	6.0mL/min	13±19.5
Reservoir → PD	4.0mL/min	16±15.3

*Table 1: Average duration of screening steps from the reservoir to the light detector at different flow rates. (0.08cm inner diameter and 88cm length)*

Step	Flow Rate (mL/min)	Time (sec)
PD → Entrapment Dock	2mL/min	12
PD → Entrapment Dock	1.75mL/min	14
PD → Entrapment Dock	1.50mL/min	16
PD → Entrapment Dock	1.25mL/min	19

*Table 2: Calculated duration of screening steps from the photo-detector to the entrapment dock at different flow rates. (0.08cm inner diameter and 80cm length)*

Step	Time (sec)
Injection procedure	User dependent: 10±3

*Table 3: Average time required for injection*

Step	5mL/min	4mL/min	3mL/min	2mL/min
Entrapment Dock → Exit	4	5	6	9

*Table 4: Calculated duration of screening steps from the entrapment dock to the exit (of the entire system) at different flow rates. (0.08cm inner diameter and 62cm length)*

### **3.5 Quantitative Assessment of Animal Health**

The condition of each individual zebrafish was assessed after it passed through the system. This assessment was based on both functional and morphological criteria. At all flow rates (2mL/min, 1.75mL/min, 1.5mL/min, 1.2mL/min), heartbeat, touch-response, structural integrity of the yolk sac and melanocytes, were evaluated and compared to a control sample. The larvae in the control setup (same age) were aspirated in an unobstructed tube spanning the length of travel encountered by larvae in the experimental setup.

#### **3.5.1 Procedure**

The zebrafish from the tests described in *section 3.4* were collected and viewed under a microscope to evaluate the following parameters: survival (heartbeat) and morphology (structural integrity of the yolk sac and melanocytes). The following data were recorded in *Figure 18*.

#### **3.5.2 Results**

At all of the flow rates used, 100% of the larvae survived (n=100) for at least. Tearing of the yolk sac was never observed. At the highest initial flow rate of 2mL/min, 48% of the larvae exhibited morphological abnormalities, specifically slight distortion of melanocytes along the tail and of the yolk extension, *Figure 18*. With the slightly slower initial aspiration rates of 1.75mL/min, all health criteria matched those of the controls.



*Figure 18: Comparison of morphological abnormalities of experimental zebrafish, at different flow rates, with a control zebrafish. The red arrows show distortions of the melanocytes and the highlighted region shows distortions of the eye and the yolk.*

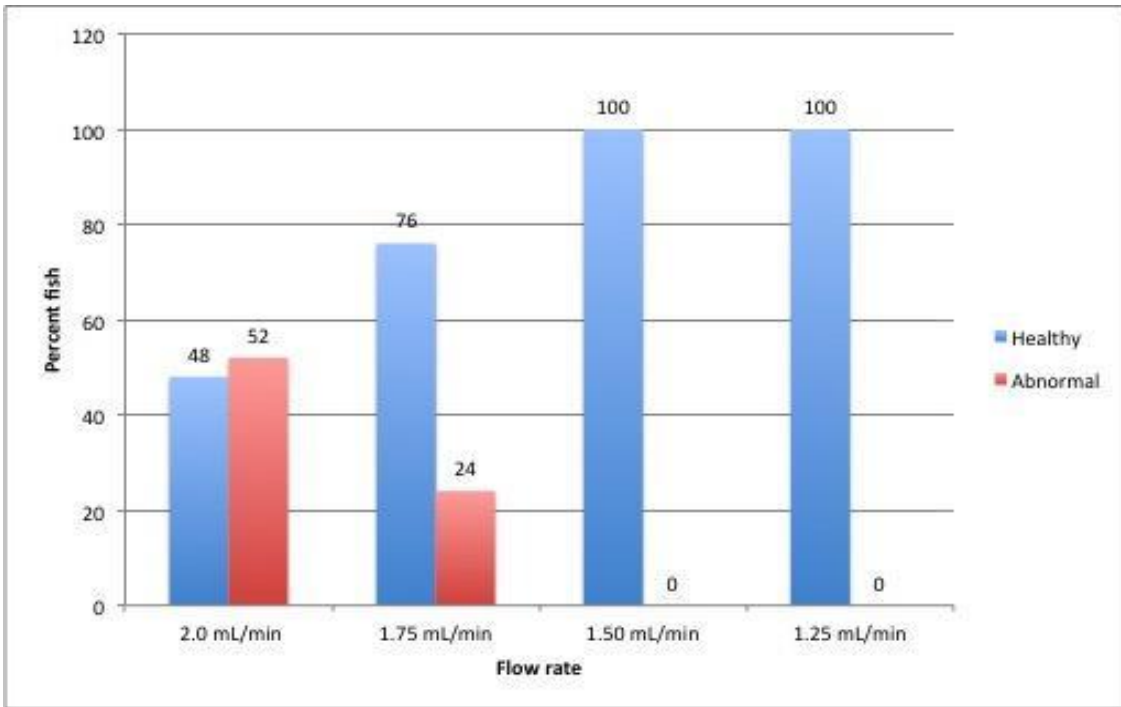


Figure 19: Quantitative assessment of zebrafish health at different flow rates (n=100)

## CHAPTER 4

### SUMMARY, CONCLUSIONS AND FUTURE WORK

#### 4.1 Summary

A device to accelerate experiments involving microinjection of large numbers of larvae was designed and fabricated using inexpensive rapid prototyping techniques. Chapter 1 introduces the influenza A virus and describes important aspects of the virus, including its genetics, distribution, transmission and clinical symptoms of the disease that it causes. This chapter also places emphasis on current IAV research advancements and reviews the use of animal models for infectious disease research. Chapter 2 describes the device components separately and reviews prototyping methods, modes of device function and supporting control software. The device specifications and parameters are also highlighted in this chapter. Chapter 3 presents efficacy tests of the main components of the system.

#### 4.2 Conclusions

A fully functional zebrafish immobilization device was designed, fabricated, and tested. 48-72 hpf zebrafish larvae were successfully immobilized within a 3D printed dock. The experimental test setup allowed manipulation of the volumetric flow rate within the tubes, pressure from the air compressor used to create air bubbles in reservoir 1, voltage within the optical detection system and the overall device output frequency. The loading stage was improved with the addition of the bubbler to reservoir 1. This played a major role in distributing larvae evenly within the chamber during operation.

Automation of the system enhanced test reproducibility by reducing the chances for human error. The optical detection system proved effective (see waveform chart, *Figure 16*). Individual larvae were successfully identified by the detection system with 100% precision (no false positives). The control software traced the recorded voltage readings that registered below the basal reading; moreover, the comparator increased the data acquisition rate two-fold, from 62 Hz to 124 Hz.

One of the most challenging aspects of the project was the fabrication of the immobilization dock. The 3D printer that was used for this project deposited support material within the channels and no method used to remove the material was successful. By developing the split design technique, I eliminated this problem by exposing the channels for simplified post-print processing. The tests of the entrapment dock were successful, i.e. after running 100 cycles through the dock at various flow rates: 48% of larvae (n=25) were immobilized without any deformation at 2mL/min, 76% of larvae (n=25) were immobilized without any deformation at 1.75mL/min, 100% of larvae (n=25) were immobilized without any deformation at 1.50mL/min, 100% of larvae (n=25) were immobilized without any deformation at 1.25mL/min.

### **4.3 Future Work**

At this stage of device development, adjusting the flow rate within the system during certain parts of a given cycle can alter the frequency of the device's output. In spite of the automation incorporated into the device, the user must manually trigger

the control program to execute certain commands such as when to inject the specimen. By adding a minimal number of steps to the existing control program, an automatic injector equipped with a translation stage could be incorporated into the design to reduce the need for manual input. Furthermore, a recovery system could easily be integrated toward the end of the device to receive the injected larvae after ejection from the system. Ultimately, the device will provide a seamless user interface that requires minimal user intervention. By depositing a known number of zebrafish larvae into the input reservoir, and inputting the dosage of the compound or chemical under study, the device will be able to inject and dispense larvae for analysis.

Microsystems designed for cell-based studies or applications such as this one require fluid handling. Flow within these systems inevitably generates fluid shear stress that may adversely affect the health of the organisms under study. Simple assays of specimen viability and morphology were used in this project to detect any gross disturbances to larval anatomy and physiology. However, it will be beneficial to specifically evaluate physiological implications of fluid shear stress within the tubes and the entrapment dock. Varma *et al.* at Massachusetts Institute of Technology explored a useful technique that can assist us with understanding the fluid dynamics within this device. It involves using a genetically encoded cell sensor that fluoresces in a quantitative fashion upon encountering fluid shear stress (FSS)<sup>98</sup>. Varma *et al.* chose a widely used cell line (NIH3T3s) and created a transcriptional cell-sensor that fluoresces when transcription of a relevant FSS-induced protein is initiated. The sensor pathway specificity and functionality were

verified by noting induced fluorescence in response to chemical induction of the FSS pathway, seen both through microscopy and flow cytometry. In addition, these novel cell sensors can be induced with a range of FSS intensities and durations, with a limit of detection of 2 dynes/cm<sup>2</sup> when applied for 30 minutes, making it more versatile in simulating several microfluidic flow conditions. Undertaking the improvements discussed above will enable for a more seamless operation of this device and possibly pave the way for subsequent engineering systems with wide applications in the microsystems community.



## BIBLIOGRAPHY

1. Yoder JA, Nielsen ME, Amemiya CT, Litman GW. Zebrafish as an immunological model system. *Microbes Infect.* 2002;4(14):1469-1478. doi:10.1016/S1286-4579(02)00029-1.
2. Gabor K a, Goody MF, Mowel WK, et al. Influenza A virus infection in zebrafish recapitulates mammalian infection and sensitivity to anti-influenza drug treatment. *Dis Model Mech.* 2014;7(11):1227-1237. doi:10.1242/dmm.014746.
3. Varki A, Gagneux P. Multifarious roles of sialic acids in immunity. *Ann N Y Acad Sci.* 2012;1253:16-36. doi:10.1111/j.1749-6632.2012.06517.x.
4. Kimmel CB, Ballard WW, Kimmel SR, Ullmann B, Schilling TF. Stages of embryonic development of the zebrafish. *Dev Dyn.* 1995;203(3):253-310. doi:10.1002/aja.1002030302.
5. Worobey M, Han G-Z, Rambaut A. A synchronized global sweep of the internal genes of modern avian influenza virus. *Nature.* 2014;508(7495):254-257. doi:10.1038/nature13016.
6. Couch RB. Orthomyxoviruses. 1996. <http://www.ncbi.nlm.nih.gov/books/NBK8611/>. Accessed May 18, 2016.
7. HILLEMANN M. Realities and enigmas of human viral influenza: pathogenesis, epidemiology and control. *Vaccine.* 2002;20(25-26):3068-3087. doi:10.1016/S0264-410X(02)00254-2.
8. Mosnier A, Caini S, Daviaud I, et al. Clinical Characteristics Are Similar across Type A and B Influenza Virus Infections. *PLoS One.* 2015;10(9):e0136186. doi:10.1371/journal.pone.0136186.
9. Lemaitre M, Carrat F. Comparative age distribution of influenza morbidity and mortality during seasonal influenza epidemics and the 2009 H1N1 pandemic. *BMC Infect Dis.* 2010;10(1):162. doi:10.1186/1471-2334-10-162.
10. Key Facts about Influenza (Flu) & Flu Vaccine | Seasonal Influenza (Flu) | CDC. <http://www.cdc.gov/flu/keyfacts.htm>. Accessed March 14, 2016.

11. Thompson WW, Shay DK, Weintraub E, et al. Influenza-associated hospitalizations in the United States. *JAMA*. 2004;292(11):1333-1340. doi:10.1001/jama.292.11.1333.
12. Fouchier RAM, Schneeberger PM, Rozendaal FW, et al. Avian influenza A virus (H7N7) associated with human conjunctivitis and a fatal case of acute respiratory distress syndrome. *Proc Natl Acad Sci U S A*. 2004;101(5):1356-1361. doi:10.1073/pnas.0308352100.
13. Hay AJ, Gregory V, Douglas AR, Lin YP. The evolution of human influenza viruses. *Philos Trans R Soc Lond B Biol Sci*. 2001;356(1416):1861-1870. doi:10.1098/rstb.2001.0999.
14. Potter CW. A history of influenza. *J Appl Microbiol*. 2001;91(4):572-579. doi:10.1046/j.1365-2672.2001.01492.x.
15. CDC Novel H1N1 Flu | The 2009 H1N1 Pandemic: Summary Highlights, April 2009-April 2010. <http://www.cdc.gov/h1n1flu/cdcresponse.htm>. Accessed May 20, 2016.
16. Laboratory-Confirmed Influenza Hospitalizations. <http://gis.cdc.gov/grasp/fluview/FluHospChars.html>. Accessed May 19, 2016.
17. No WV. Estimates of deaths associated with seasonal influenza --- United States, 1976-2007. *MMWR Morb Mortal Wkly Rep*. 2010;59(33):1057-1062. doi:mm5933a1 [pii].
18. Prevention and Control of Influenza with Vaccines. <http://www.cdc.gov/mmwr/preview/mmwrhtml/rr59e0729a1.htm>. Accessed May 19, 2016.
19. Flu Transmission. <https://www.niaid.nih.gov/topics/flu/understandingflu/Pages/transmission.aspx>. Accessed May 20, 2016.
20. Thomas Y, Vogel G, Wunderli W, et al. Survival of influenza virus on banknotes. *Appl Environ Microbiol*. 2008;74(10):3002-3007. doi:10.1128/AEM.00076-08.

21. Thomas Y, Boquete-Suter P, Koch D, Pittet D, Kaiser L. Survival of influenza virus on human fingers. *Clin Microbiol Infect.* 2014;20(1). doi:10.1111/1469-0691.12324.
22. P. Sivaramakrishna Rachakonda: STUDIES ON CONFORMATIONAL STABILITY OF THE ECTODOMAIN OF INFLUENZA VIRUS HEMAGGLUTININ. <http://edoc.hu-berlin.de/dissertationen/rachakonda-p-sivaramakrishna-2005-02-15/HTML/chapter1.html>. Accessed May 20, 2016.
23. Pneumonia Symptoms & Treatment | Cleveland Clinic. [http://my.clevelandclinic.org/health/diseases\\_conditions/hic\\_Pneumonia](http://my.clevelandclinic.org/health/diseases_conditions/hic_Pneumonia). Accessed May 20, 2016.
24. Medina R a, García-Sastre A. Influenza A viruses: new research developments. *Nat Rev Microbiol.* 2011;9(8):590-603. doi:10.1038/nrmicro2613.
25. Nicholson KG, Wood JM, Zambon M. Influenza. *Lancet (London, England).* 2003;362(9397):1733-1745. doi:10.1016/S0140-6736(03)14854-4.
26. Tsai KN, Chen GW. Influenza genome diversity and evolution. *Microbes Infect.* 2011;13(5):479-488. doi:10.1016/j.micinf.2011.01.013.
27. Kanekiyo M, Wei C-J, Yassine HM, et al. Self-assembling influenza nanoparticle vaccines elicit broadly neutralizing H1N1 antibodies. *Nature.* 2013;499(7456):102-106. doi:10.1038/nature12202.
28. Melcher L. Recommendations for influenza and pneumococcal vaccinations in people receiving chemotherapy. *Clin Oncol.* 2005;17(1):12-15. doi:10.1016/j.clon.2004.07.010.
29. Taubenberger JK, Morens DM. The pathology of influenza virus infections. *Annu Rev Pathol.* 2008;3:499-522. doi:10.1146/annurev.pathmechdis.3.121806.154316.
30. Pardo-Martin C, Chang T-Y, Koo BK, Gilleland CL, Wasserman SC, Yanik MF. High-throughput in vivo vertebrate screening. *Nat Methods.* 2010;7(8):634-636. doi:10.1038/nmeth.1481.

31. Flu (Influenza) Basic Research.  
<https://www.niaid.nih.gov/topics/Flu/Research/basic/Pages/default.aspx>.  
Accessed May 23, 2016.
32. Genome Sequencing Centers.  
<http://www.niaid.nih.gov/labsandresources/resources/dmid/gsc/influenza/Pages/default.aspx>. Accessed May 23, 2016.
33. Davidson JM. Animal models for wound repair. *Arch Dermatol Res*. 1998;290(14):S1-S11. doi:10.1007/PL00007448.
34. Lee KY, DeMayo FJ. Animal models of implantation. *Reproduction*. 2004;128(6):679-695. doi:10.1530/rep.1.00340.
35. Brown L, Panchal SK. Rodent models for metabolic syndrome research. *J Biomed Biotechnol*. 2011;2011. doi:10.1155/2011/351982.
36. Johnson T V., Tomarev SI. Rodent models of glaucoma. *Brain Res Bull*. 2010;81(2-3):349-358. doi:10.1016/j.brainresbull.2009.04.004.
37. The Use of Animal Models in Studying Genetic Disease.  
<http://www.nature.com/scitable/topicpage/the-use-of-animal-models-in-studying-855>. Accessed May 25, 2016.
38. Bouvier NM, Lowen AC. Animal Models for Influenza Virus Pathogenesis and Transmission. *Viruses*. 2010;2(8):1530-1563. doi:10.3390/v20801530.
39. Trede NS, Langenau DM, Traver D, Look AT, Zon LI. The use of zebrafish to understand immunity. *Immunity*. 2004;20(4):367-379. doi:10.1016/S1074-7613(04)00084-6.
40. Van Der Sar AM, Appelmeik BJ, Vandenbroucke-Grauls CMJE, Bitter W. A star with stripes: Zebrafish as an infection model. *Trends Microbiol*. 2004;12(10):451-457. doi:10.1016/j.tim.2004.08.001.
41. Sullivan C, Kim CH. Zebrafish as a model for infectious disease and immune function. *Fish Shellfish Immunol*. 2008;25(4):341-350. doi:10.1016/j.fsi.2008.05.005.

42. Robertson GN, McGee CAS, Dumbarton TC, Croll RP, Smith FM. Development of the swimbladder and its innervation in the zebrafish, *Danio rerio*. *J Morphol*. 2007;268(11):967-985. doi:10.1002/jmor.10558.
43. Gratacap RL, Rawls JF, Wheeler RT. Mucosal candidiasis elicits NF- $\kappa$ B activation, proinflammatory gene expression and localized neutrophilia in zebrafish. *Dis Model Mech*. 2013;6(5):1260-1270. doi:10.1242/dmm.012039.
44. Zheng W, Wang Z, Collins JE, Andrews RM, Stemple D, Gong Z. Comparative transcriptome analyses indicate molecular homology of zebrafish swimbladder and mammalian lung. *PLoS One*. 2011;6(8):e24019. doi:10.1371/journal.pone.0024019.
45. Winata CL, Korzh S, Kondrychyn I, Zheng W, Korzh V, Gong Z. Development of zebrafish swimbladder: The requirement of Hedgehog signaling in specification and organization of the three tissue layers. *Dev Biol*. 2009;331(2):222-236. doi:10.1016/j.ydbio.2009.04.035.
46. Lam S., Chua H., Gong Z, Lam T., Sin Y. Development and maturation of the immune system in zebrafish, *Danio rerio*: a gene expression profiling, in situ hybridization and immunological study. *Dev Comp Immunol*. 2004;28(1):9-28. doi:10.1016/S0145-305X(03)00103-4.
47. Meeker ND, Trede NS. Immunology and zebrafish: Spawning new models of human disease. *Dev Comp Immunol*. 2008;32(7):745-757. doi:10.1016/j.dci.2007.11.011.
48. Trede NS, Langenau DM, Traver D, Look AT, Zon LI. The use of zebrafish to understand immunity. *Immunity*. 2004;20(4):367-379. <http://www.ncbi.nlm.nih.gov/pubmed/15084267>. Accessed December 2, 2016.
49. Dobson JT, Seibert J, Teh EM, et al. Carboxypeptidase A5 identifies a novel mast cell lineage in the zebrafish providing new insight into mast cell fate determination. *Blood*. 2008;112(7).
50. Kanther M, Rawls JF. Host-microbe interactions in the developing zebrafish. *Curr Opin Immunol*. 2010;22(1):10-19. doi:10.1016/j.coi.2010.01.006.

51. Encinas P, Rodriguez-Milla MA, Novoa B, Estepa A, Figueras A, Coll J. Zebrafish fin immune responses during high mortality infections with viral haemorrhagic septicemia rhabdovirus. A proteomic and transcriptomic approach. *BMC Genomics*. 2010;11:518. doi:10.1186/1471-2164-11-518.
52. Burgos JS, Ripoll-Gomez J, Alfaro JM, Sastre I, Valdivieso F. Zebrafish as a new model for herpes simplex virus type 1 infection. *Zebrafish*. 2008;5(4):323-333. doi:10.1089/zeb.2008.0552.
53. Manicassamy B, Manicassamy S, Belicha-Villanueva A, Pisanelli G, Pulendran B, García-Sastre A. Analysis of in vivo dynamics of influenza virus infection in mice using a GFP reporter virus. *Proc Natl Acad Sci U S A*. 2010;107(25):11531-11536. doi:10.1073/pnas.0914994107.
54. Hemagglutinin. <http://www.sinobiological.com/Influenza-Hemagglutinin-Function-a-147.html>.
55. Ito T, Couceiro JN, Kelm S, et al. Molecular basis for the generation in pigs of influenza A viruses with pandemic potential. *J Virol*. 1998;72(9):7367-7373. <http://www.ncbi.nlm.nih.gov/pubmed/9696833>. Accessed November 14, 2016.
56. Leung HSY, Li OTW, Chan RWY, Chan MCW, Nicholls JM, Poon LLM. Entry of influenza A Virus with a  $\alpha$ 2,6-linked sialic acid binding preference requires host fibronectin. *J Virol*. 2012;86(19):10704-10713. doi:10.1128/JVI.01166-12.
57. Lakadamyali M, Rust MJ, Zhuang X. Endocytosis of influenza viruses. *Microbes Infect*. 2004;6(10):929-936. doi:10.1016/j.micinf.2004.05.002.
58. Chu VC, Whittaker GR. Influenza virus entry and infection require host cell N-linked glycoprotein. *Proc Natl Acad Sci U S A*. 2004;101(52):18153-18158. doi:10.1073/pnas.0405172102.
59. de Vries E, de Vries RP, Wienholts MJ, et al. Influenza A virus entry into cells lacking sialylated N-glycans. *Proc Natl Acad Sci U S A*. 2012;109(19):7457-7462. doi:10.1073/pnas.1200987109.

60. de Vries E, Tscherne DM, Wienholts MJ, et al. Dissection of the Influenza A Virus Endocytic Routes Reveals Macropinocytosis as an Alternative Entry Pathway. Pekosz A, ed. *PLoS Pathog.* 2011;7(3):e1001329. doi:10.1371/journal.ppat.1001329.
61. Karlsson Hedestam GB, Fouchier RAM, Phogat S, Burton DR, Sodroski J, Wyatt RT. The challenges of eliciting neutralizing antibodies to HIV-1 and to influenza virus. *Nat Rev Microbiol.* 2008;6(2):143-155. doi:10.1038/nrmicro1819.
62. Oguin TH, Sharma S, Stuart AD, et al. Phospholipase D Facilitates Efficient Entry of Influenza Virus, Allowing Escape from Innate Immune Inhibition. *J Biol Chem.* 2014;289(37):25405-25417. doi:10.1074/jbc.M114.558817.
63. Crim MJ, Riley LK. Viral diseases in zebrafish: what is known and unknown. *ILAR J.* 2012;53(2):135-143. doi:10.1093/ilar.53.2.135.
64. Marx M, Rutishauser U, Bastmeyer M. Dual function of polysialic acid during zebrafish central nervous system development. *Development.* 2001;128(24):4949-4958. <http://www.ncbi.nlm.nih.gov/pubmed/11748132>. Accessed November 14, 2016.
65. Dehnert KW, Baskin JM, Laughlin ST, et al. Imaging the sialome during zebrafish development with copper-free click chemistry. *Chembiochem.* 2012;13(3):353-357. doi:10.1002/cbic.201100649.
66. Langhauser M, Ustinova J, Rivera-Milla E, et al. Ncam1a and Ncam1b: two carriers of polysialic acid with different functions in the developing zebrafish nervous system. *Glycobiology.* 2012;22(2):196-209. doi:10.1093/glycob/cwr129.
67. Neu U, Bauer J, Stehle T. Viruses and sialic acids: rules of engagement. *Curr Opin Struct Biol.* 2011;21(5):610-618. doi:10.1016/j.sbi.2011.08.009.
68. Matrosovich M, Herrler G, Klenk HD. Sialic Acid Receptors of Viruses. In: Springer International Publishing; 2013:1-28. doi:10.1007/128\_2013\_466.

69. M M, A T, N B, et al. Early alterations of the receptor-binding properties of H1, H2, and H3 avian influenza virus hemagglutinins after their introduction into mammals. *J Virol.* 2000;74.
70. Levy DE, Garcí#a-Sastre A. The virus battles: IFN induction of the antiviral state and mechanisms of viral evasion. *Cytokine Growth Factor Rev.* 2001;12(2):143-156. doi:10.1016/S1359-6101(00)00027-7.
71. Goodbourn S, Didcock L, Randall RE. Interferons: Cell signalling, immune modulation, antiviral responses and virus countermeasures. 2000;81(10):2341-2364.
72. Schindler C, Brutsaert S. Interferons as a paradigm for cytokine signal transduction. 1999;55(12):1509-1522. doi:10.1007/s000180050391.
73. Herbomel P, Thisse B, Thisse C. Ontogeny and behaviour of early macrophages in the zebrafish embryo. *Development.* 1999;126(17):3735-3745. <http://www.ncbi.nlm.nih.gov/pubmed/10433904>. Accessed December 13, 2016.
74. Le Guyader D, Redd MJ, Colucci-Guyon E, et al. Origins and unconventional behavior of neutrophils in developing zebrafish. *Blood.* 2008;111(1):132-141. doi:10.1182/blood-2007-06-095398.
75. Willett CE, Cherry JJ, Steiner LA. Characterization and expression of the recombination activating genes (rag1 and rag2) of zebrafish. *Immunogenetics.* 1997;45(6):394-404. <http://www.ncbi.nlm.nih.gov/pubmed/9089097>. Accessed December 13, 2016.
76. Danilova N, Steiner LA. B cells develop in the zebrafish pancreas. *Proc Natl Acad Sci U S A.* 2002;99(21):13711-13716. doi:10.1073/pnas.212515999.
77. Lam SH, Chua HL, Gong Z, Lam TJ, Sin YM. Development and maturation of the immune system in zebrafish, *Danio rerio*: a gene expression profiling, in situ hybridization and immunological study. *Dev Comp Immunol.* 2004;28(1):9-28. <http://www.ncbi.nlm.nih.gov/pubmed/12962979>. Accessed December 13, 2016.



78. Dirscherl H, McConnell SC, Yoder JA, de Jong JLO. The MHC class I genes of zebrafish. *Dev Comp Immunol*. 2014;46(1):11-23. doi:10.1016/j.dci.2014.02.018.
79. Takeuchi H, Figueroa F, O'hUigin C, Klein J. Cloning and characterization of class I Mhc genes of the zebrafish, *Brachydanio rerio*. *Immunogenetics*. 1995;42:77-84. doi:10.1007/BF00178581.
80. Rosen JN, Sweeney MF, Mably JD. Microinjection of zebrafish embryos to analyze gene function. *J Vis Exp*. 2009;(25):2-5. doi:10.3791/1115.
81. Tips and Tricks for the Lab: How to Make a Capillary TLC Spotter :: Education :: ChemistryViews. [http://www.chemistryviews.org/details/education/2102991/Tips\\_and\\_Tricks\\_for\\_the\\_Lab\\_How\\_to\\_Make\\_a\\_Capillary\\_TLC\\_Spotter.html](http://www.chemistryviews.org/details/education/2102991/Tips_and_Tricks_for_the_Lab_How_to_Make_a_Capillary_TLC_Spotter.html). Accessed January 3, 2017.
82. Kardash E. Current Methods in Zebrafish Research. *Mater Methods*. 2012;2. doi:10.13070/mm.en.2.109.
83. Cui C, Benard EL, Kanwal Z, et al. Infectious Disease Modeling and Innate Immune Function in Zebrafish Embryos. In: *Methods in Cell Biology*. Vol 105. ; 2011:273-308. doi:10.1016/B978-0-12-381320-6.00012-6.
84. Technological Progress - Our World In Data. <https://ourworldindata.org/technological-progress/>. Accessed January 11, 2017.
85. Alhnan MA, Okwuosa TC, Sadia M, Wan K-W, Ahmed W, Arafat B. Emergence of 3D Printed Dosage Forms: Opportunities and Challenges. *Pharm Res*. 2016;33(8):1817-1832. doi:10.1007/s11095-016-1933-1.
86. 3D Printing Industry Examples and Case Studies. <http://www.javelin-tech.com/3d-printer/industry/>. Accessed January 15, 2017.
87. Surgeon's Helper: 3D Printing Is Revolutionizing Health Care. <http://www.livescience.com/49913-3d-printing-revolutionizing-health-care.html>. Accessed January 15, 2017.

88. Rengier F, Mehndiratta A, von Tengg-Kobligk H, et al. 3D printing based on imaging data: review of medical applications. *Int J Comput Assist Radiol Surg.* 2010;5(4):335-341. doi:10.1007/s11548-010-0476-x.
89. Alternate Immobilization technique- MF channels/Suction. <http://www.pnas.org.prxy4.ursus.maine.edu/content/104/35/13891.full.pdf> . Accessed March 19, 2016.
90. Bischel LL, Mader BR, Green JM, Huttenlocher A, Beebe DJ. Zebrafish Entrapment By Restriction Array (ZEBRA) device: a low-cost, agarose-free zebrafish mounting technique for automated imaging. *Lab Chip.* 2013;13(9):1732-1736. doi:10.1039/c3lc50099c.
91. Resto PJ, Mogen B, Wu F, Berthier E, Beebe D, Williams J. High speed droplet-based delivery system for passive pumping in microfluidic devices. *J Vis Exp.* 2009;(31):3-7. doi:10.3791/1329.
92. Westhoff JH, Giselbrecht S, Schmidts M, et al. Development of an Automated Imaging Pipeline for the Analysis of the Zebrafish Larval Kidney. Hwang S-PL, ed. *PLoS One.* 2013;8(12):e82137. doi:10.1371/journal.pone.0082137.
93. VeroClear, RGD810 | Flavors | NA | Materials & Accessories | Stratasys eStore. <https://store.stratasys.com/stratasysstorefront/stratasys/en/USD/Materials-%26-Accessories/NA/Flavors/VeroClear%2C-RGD810/p/P030>. Accessed February 22, 2017.
94. Bio Compatible, MED610 | Flavors | NA | Materials & Accessories | Stratasys eStore. <https://store.stratasys.com/stratasysstorefront/stratasys/en/USD/Materials-%26-Accessories/NA/Flavors/Bio-Compatible%2C-MED610/p/P015>. Accessed February 22, 2017.
95. Macdonald NP, Zhu F, Hall CJ, et al. Assessment of biocompatibility of 3D printed photopolymers using zebrafish embryo toxicity assays. *Lab Chip.* 2016;16(2):291-297. doi:10.1039/c5lc01374g.
96. Oskui SM, Diamante G, Liao C, et al. Assessing and Reducing the Toxicity of 3D-Printed Parts. *Environ Sci Technol Lett.* 2016;3(1):1-6. doi:10.1021/acs.estlett.5b00249.

97. Ho CMB, Ng SH, Li KHH, Yoon Y-J. 3D printed microfluidics for biological applications. *Lab Chip*. 2015;15(18):3627-3637. doi:10.1039/c5lc00685f.
98. Varma S, Voldman J. A cell-based sensor of fluid shear stress for microfluidics. *Lab Chip*. 2015;15(6):1563-1573. doi:10.1039/c4lc01369g.
99. Phennicie RT, Sullivan MJ, Singer JT, Yoder JA, Kim CH. Specific resistance to *Pseudomonas aeruginosa* infection in zebrafish is mediated by the cystic fibrosis transmembrane conductance regulator. *Infect Immun*. 2010;78(11):4542-4550. doi:10.1128/IAI.00302-10.
100. ZFIN The Zebrafish Model Organism Database. <http://zfin.org/>. Accessed March 22, 2017.

## APPENDIX A

### ZEBRAFISH HUSBANDRY

Zebrafish were housed at the University of Maine Zebrafish Facility in recirculating systems where the water temperature was maintained at 28°C with a total system flow rate of 150 liters/min. Zebrafish were maintained in accordance with the Institutional Animal Care and Use Committee standards of the University of Maine. Fertilized zebrafish eggs are collected according to methods proposed by Phennecie at the University of Maine Zebrafish Facility<sup>99</sup>. Collected eggs are raised for 24 hours at 28.0°C in 100mm-diameter petri dishes half full of egg water, 60µg/L Instant Ocean Salts in purified reverse osmosis water. No more than 100 eggs were raised in one 100mm-diameter petri dish at a time.

At 24 hours post fertilization, egg water is replaced in each petri dish. Chorions are removed from the embryos by hand and discarded as biological waste. Live embryos are stored at 28.0°C until the following day.

At 48hpf, embryos are motile. Egg water is replaced in each petri dish and dead embryos are removed from the container. Embryos are stored at 28.0°C overnight.

At 72hpf, specimens are considered larvae. Zebrafish egg water is replaced and specimens are used as needed in further laboratory procedures.

Zebrafish were euthanized in a 600µg/L concentrated stock of Tricane for 30min and fixed to minimize the amount of larvae needed for repeated testing. Fish are removed from anesthetic and placed in fixative solution of 1.5% gluteraldehyde, 0.5% para-formaldehyde, 50mM PBS (phosphate buffered saline) for long term storage<sup>100</sup>. Larvae were fixed for at least 12 hours prior to use. For flow testing,

chemically fixed fish were removed from fixative solution and placed in egg water with no more than 0.25% gelatin to minimize larval adhesion to tubing.

For procedures involving live specimens, larvae are anaesthetized in a 200µg/mL solution of tricane with no more than 0.25% gelatin added to minimize specimen adhesion to tubing. Fish were aspirated through the device in the anesthetic gelatin solution.

## APPENDIX B

### VALVE/SYRINGE PUMP CONTROL MAP

#### SETUP:

MyDAQ DIO channels (0-5)

- Input – laser detector (detected fish=1, nothing detected=0)
- Output – valve 1 (open=1, close=0)
- Output – valve 2 (open=1, close=0)
- Output – valve 3 (open=1, close=0)
- Output – valve 4 (open=1, close=0)
- Output – valve 5 (open=1, close=0)
- Output – syringe pump direction (inject=1, withdraw=0)
- Output – syringe pump start/stop (start=1, stop=0)

#### Program Commands:

- All valves closed, pump stopped
- Set pump to withdraw mode
- Close valve 2, Close valve 4, Close valve 5(should be closed already)
- Open valve 1 and valve 3
- Start pump 1
- Monitor detector
- If positive detect → stop pump, close valve 1, close valve 3, open valve 2, open valve 3 set pump to inject, start pump
- Pump injects. Duration: (input value) seconds → stop pump, valve 2 close

- Inject. Duration: (input value) seconds
- Open valve 4, open valve 5
- Start pump 2 (infuse)
- Wait for fish to flush out. Duration: (input value) seconds
- Stop pump
- Close valve 5
- Go to Step 1

## APPENDIX C

### MATERIALS LIST

#### Pump System Materials:

- Tygon Micro Bore Tubing, Part #: TGY-030. Component Supply Co.
- Silicone Tubing, Part #: SCT-063A. Component Supply Co.
- BD 60mL Syringe, Part #: 309654. Becton, Dickinson and Company.
- New Era NE-1000X Programmable Syringe Pump
- 2-way normally closed solenoid pinch valve, Part # 98302. Cole Palmer Instrument Company, LLC.
- Aqua Culture Single Outlet Aquarium Air Pump, Part # 0079285405132

#### Optical Detection Materials

- 5mm transparent cylinder head photodiode, Part # LLS05-A. Senba Optical Electrical Co., Ltd
- 4.5V 650 nm red laser diode module, Part # 01444878. LightInTheBox Co., Ltd
- PROCELL 1.5V dry cell batteries, Part # PC1500. Duracell Inc.

#### Entrapment Dock Materials

- Objet30 Rapid Prototyping System, SUP705 Support Material (Water Jet Removable). Stratasys Ltd.
- Custom Stage Mount
- MakerBot Replicator Desktop 3D Printer, PLA Filament. MakerBot Industries, LLC.



## Electronics

- National Instruments myDAQ Unit
- SC5 Five-Channel Solenoid Controller/Driver. RW Automations, LLC.
- SolidEdge ST7. Siemens Product Lifecycle Management Software Inc.
- National Instruments LabVIEW 2016. National Instruments.

## **BIOGRAPHY OF THE AUTHOR**

Fuoad Saliou-Sulley was born in Accra, Ghana on 16<sup>th</sup> July 1991. He lived with his family and attended school in Accra till he was 17, when he came to the United States as an exchange student. Fuoad lived with a host family in Kennebunkport, ME and graduated from Kennebunk High School in 2009. In May 2014, he graduated Magna Cum Laude from the University of Maine in Orono with a degree in Biology and a minor in Chemistry. In the fall of 2014, he enrolled in the school of Chemical and Biological Engineering at the University of Maine doing research in the laboratory of Dr. Paul J. Millard.

Fuoad intends to continue pursuing scientific research studies, particularly in a biomedical or pharmaceutical institution. Whenever he has a chance to, Fuoad likes to spend time with friends. He is also very fond of outdoor sports and activities like hiking, mountain biking, soccer and basketball. He is a candidate for the Master of Science degree in Biological Engineering from the University of Maine in August 2017.